Atmos. Meas. Tech. Discuss., doi:10.5194/amt-2015-351, 2016
Manuscript under review for journal Atmos. Meas. Tech.
Published: 1 February 2016

Atmospheric Measurement Techniques Discussions

A new setup for simultaneous high precision measurements of CO_2, $\delta^{13}C$-CO_2 and $\delta^{18}O$-CO_2 on small ice core samples

T. M. Jenk[1,*], M. Rubino[2,#], D. Etheridge[2], V. G. Ciobanu[1], T. Blunier[1]

[1]{Centre for Ice and Climate, Niels Bohr Institute, University of Copenhagen, Copenhagen, Denmark}

[2]{CSIRO Oceans and Atmosphere, Aspendale, Victoria, Australia}

[*]{now at: Paul Scherrer Institut, Laboratory for Radio– and Environmental Chemistry, Villigen PSI, Switzerland}

[#]{now at: Seconda Università degli Studi di Napoli, Caserta, Italy}

Correspondence to: T. M. Jenk (theo.jenk@psi.ch)

Atmos. Meas. Tech. Discuss., doi:10.5194/amt-2015-351, 2016
Manuscript under review for journal Atmos. Meas. Tech.
Published: 1 February 2016

Atmospheric Measurement Techniques Discussions

Abstract

Paleo–atmospheric records of carbon dioxide and its stable carbon isotope composition ($\delta^{13}C$) obtained from polar ice cores provide important constraints on the natural variability of the carbon cycle. However, the measurements are both analytically challenging and time-consuming thus data exist only from a limited number of sampling sites and time periods. Additional analytical resources with high analytical precision and throughput are thus desirable to extend and confirm the existing datasets. Also, consistent measurements derived by independent laboratories and a variety of analytical systems helps to further increase confidence in the global CO_2 paleo reconstructions. Here, we describe our new setup for simultaneous measurements of atmospheric CO_2 mixing ratios, atmospheric $\delta^{13}C$ and $\delta^{18}O$-CO_2 in air extracted from ice core samples. The core of the system is a newly designed Needle Cracker for the mechanical release of air entrapped in ice core samples of 8–13 g operated at -45 °C. The small sample size allows for high resolution and replicate sampling schemes. In our method, CO_2 is cryogenically and chromatographically separated from the bulk air and the isotopic composition subsequently determined by continuous flow isotope ratio mass spectrometry (IRMS). In combination with thermal conductivity measurement of the bulk air, the CO_2 mixing ratio is calculated. The analytical precision determined from standard air sample measurements over ice is ± 1.9 ppm for CO_2 and ± 0.09 ‰ for $\delta^{13}C$. In a laboratory intercomparison study with CSIRO (Aspendale, Australia) good agreement between CO_2 and $\delta^{13}C$ results is found for Law Dome ice core samples. Replicate analysis of these samples resulted in a pooled standard deviation of 2.0 ppm for CO_2 and 0.11 ‰ for $\delta^{13}C$. These numbers are good, although rather conservative estimates of the overall analytical uncertainty for a single measurement. Facilitated by the small sample requirement, replicate measurements are feasible and the achievable method precision accordingly higher. Further in this study, new analytical approaches are introduced for the accurate correction of the procedural blank and for the reliable and consistent detection of measurement outliers which is based on $\delta^{18}O$-CO_2 and the exchange of oxygen between CO_2 and H_2O of surrounding ice.

Atmos. Meas. Tech. Discuss., doi:10.5194/amt-2015-351, 2016
Manuscript under review for journal Atmos. Meas. Tech.
Published: 1 February 2016

Atmospheric Measurement Techniques Discussions

1 Introduction

Polar ice cores are unique in providing direct information of the past atmospheric composition. Analyses of entrapped air allows to reconstruct the evolution of the atmospheric composition over the last 800,000 years (e.g. Lüthi et al., 2008 and references therein; Bereiter et al., 2015). Profound knowledge of past natural CO_2 variations – only several ppm during the Holocene and up to about 100 ppm over glacial/interglacial changes – is crucial to improve and better constrain predictions of future climate under continued anthropogenic CO_2 forcing. Changes in the global carbon cycle fluxes are imprinted in the stable carbon isotope signal of atmospheric CO_2 ($\delta^{13}C$, e.g. Köhler et al., 2006). However, carbon isotope measurements of ice core air samples are highly demanding and time consuming. As a result, detailed measurements of $\delta^{13}C$ are still limited to specific time periods (Francey et al., 1999; Indermühle et al., 1999; Smith et al., 1999; Elsig et al., 2009; Lourantou et al., 2010a; Lourantou et al., 2010b; Rubino et al., 2013; Schneider et al., 2013).

Since the pioneer CO_2 measurements in the 1980s (Berner et al., 1980; Delmas et al., 1980; Neftel et al., 1982; Pearman et al., 1986), extraction and measurement techniques have been continuously developed and improved, thereby constantly increasing analytical precision and accuracy. The initial step of extracting air entrapped in ice is crucial. While extraction of gas by melting the ice is successfully applied for trace gases like CH_4, CO_2 measurements are generally not reliable in the presence of liquid water (Kawamura et al., 2003). Measurement artefacts arise due to the high solubility of CO_2 and chemical reactions of carbonate species in water (Anklin et al., 1995; Zhang et al., 1995; Kawamura et al., 2003). Further challenges arise from sorption and contamination effects at surfaces particularly in connection with mechanical friction between system components (e.g. Zumbrunn et al., 1982) and common for high vacuum applications from system leakage, outgasing materials and introduction of contaminants (e.g. drilling fluid). In order to avoid the liquid phase of water, the air must either be extracted mechanically – referred to as dry or mechanical extraction – or by sublimation of the ice matrix below the triple point of water.

When the enclosed air is available in the form of bubbles the gas extraction efficiency for mechanical systems varies between 60 % and ~90 %. However, in deeper strata where the gas is present in air hydrates (e.g. Uchida et al., 1994) – also called clathrates – extraction efficiencies generally decrease by 10–20 % (less for the centrifugal ice microtome, CIM, Bereiter et al., 2013b). It has been found that in the transition zone, where air bubbles and clathrates coexist, CO_2 is enriched in clathrates and depleted in air bubbles. In this zone,

Atmos. Meas. Tech. Discuss., doi:10.5194/amt-2015-351, 2016
Manuscript under review for journal Atmos. Meas. Tech.
Published: 1 February 2016

Atmospheric Measurement Techniques Discussions

measurements of CO_2 mixing ratios can thus be severely biased as they depend on the gas extraction efficiency (Ikeda et al., 1999; Sowers and Jubenville, 2000; Ahn et al., 2009; Schaefer et al., 2011; Bereiter et al., 2013a). This problem can be avoided by sublimation of the ice matrix resulting in close to 100 % extraction efficiency (Güllük et al., 1998; Schmitt et al., 2011). Anyhow, while CO_2 concentration measurements by mechanical extraction systems are affected in the transition zone from bubble to clathrate ice, only a decrease in precision but no systematic effect could be observed for $\delta^{13}C$ analysis of CO_2 (Schaefer et al., 2011 and references therein). Also, for pure bubbly ice, the extraction efficiency is not a concern for CO_2 measurements. No difference has been observed compared to results derived by sublimation systems for which the main drawback is the much slower extraction process which limits sample throughput.

A variety of mechanical extraction systems are in use. In a Needle Cracker (NC) the ice is crushed to small pieces and air is released from the thereby opened bubbles (Zumbrunn et al., 1982). The CIM described by Bereiter et al. (2013b) pulverizes ice samples by continuously shaving off thin layers of the sample surface by a centrifugal ice microtome. Alternatively, ice samples are ground in a Ball Mill when both the ice sample and stainless steel balls inside a small container are shaken (Barnola et al., 1995; Lourantou, 2009), or grated into small chips by shaking the ice in a vessel containing a perforated inner cylinder (Cheese Grater, Etheridge et al., 1996).

Only a few laboratories have the ability to do ice core analysis of both, CO_2 and its stable isotopic composition. An overview of the presently operated and published setups allowing analysis of both parameters is given in the following. All systems use isotopic ratio mass spectrometry (IRMS) to detect the different mass ratios between the stable CO_2 isotopologues (mz 44, 45 and 46). The laboratory of the Climate and Environmental Phyiscs (KUP, Bern, Switzerland) operates two systems, one based on the mechanical extraction and the other on the sublimation principle. For the mechanical extraction by a NC the efficiency is about 70 % and 50 % for bubbly and clathrate ice, respectively. The operating temperature has been reported at -20 °C but was lowered to -35 °C since. The released air is first expanded over a water trap into a small volume where the gas pressure is measured for evaluation of the CO_2 concentration in combination with the IRMS signal. Using Helium as carrier gas, the gas sample is then flushed into a pre-concentration system (PreCon) to separate the main components of air. In order to avoid isobaric interference, CO_2 is separated from N_2O and organic compounds (e.g. from drilling fluids) by gas chromatography (GC) before being

Atmos. Meas. Tech. Discuss., doi:10.5194/amt-2015-351, 2016
Manuscript under review for journal Atmos. Meas. Tech.
Published: 1 February 2016

Atmospheric Measurement Techniques Discussions

injected into the IRMS via an open-split. The precision (always given as 1σ) is ~2.0 ppm and 0.07 ‰ for CO_2 and $\delta^{13}C$, respectively. The required sample size is small (5–6 g) and the system has a throughput of 3–6 samples per day (Elsig et al., 2009; Leuenberger, 2009). For the sublimation system the extraction efficiency is close to 100 % independent of the ice properties. The sublimated water is quantitatively removed before the liberated air is cryogenically collected. Then, the basic principle is similar to the system described before but extraction and GC–IRMS are decoupled. The precision of this method is ~2.0 ppm for CO_2 and 0.05 ‰ for $\delta^{13}C$. The sample size required is larger (~30 g) and due to the slow sublimation process the throughput is only 1–2 samples per day (Schmitt et al., 2011). In addition, KUP operates two systems (NC and CIM) solely dedicated to CO_2 concentration measurements (Zumbrunn et al., 1982; Lüthi, 2009; Bereiter et al., 2013b). At the Laboratoire de Glaciologie et Géophysique de l' Environnement (LGGE, Grenoble, France), the extraction efficiency for bubbly ice is around 70 % with the Ball Mill operated at -65 °C. It is not reported for the clathrate ice. After extraction, the air is directly released to the inlet system of a coupled GC–IRMS. The reported precision is 1.5 ppm for CO_2 and 0.1‰ for $\delta^{13}C$. The required sample size is relatively small at around 40–50 g and the throughput rather low with 1–2 samples per day (Barnola et al., 1995; Lourantou, 2009). The ice core and quaternary geochemistry lab at Oregon State University (OSU, USA) runs a system based on the Cheese Grater design operated at -60 °C. The extraction efficiency is around 60 % for bubbly ice and lower for clathrate ice. A small aliquot of the sample gas is isolated from the grater and finally trapped at -260 °C after water is removed at -100 °C. The CO_2 mixing ratio is then determined by GC with a precision of 2 ppm. The rest of the gas, again first passing a water trap at -100 °C, is condensed in a second trap at -190 °C and finally analyzed for $\delta^{13}C$ by IRMS Dual–Inlet measurement. A high precision of 0.02 ‰ is achieved with a rather large sample mass of 400–550 g required (Bauska et al., 2014). OSU also operates an additional NC system for the measurements of CO_2 only (Ahn et al., 2009). At CSIRO a Cheese Grater (-20 °C) is used for CO_2 and $\delta^{13}C$ analysis. The extraction efficiency is 60–80 % (Rubino M., pers. communication). Here, the released air is cryogenically collected at -260 °C in an external trap after removing water at -100 °C. Subsequently, the sample is analyzed with a GC for CO_2 concentration measurement and by IRMS for $\delta^{13}C$ without further GC separation and purification. A correction for the isobaric N_2O interference is applied. Interference from drilling fluid contamination can be problematic for certain samples. The precision achieved for this setup is high with 1.0 ppm for CO_2 and around 0.04 ‰ for $\delta^{13}C$. For the combined

Atmos. Meas. Tech. Discuss., doi:10.5194/amt-2015-351, 2016
Manuscript under review for journal Atmos. Meas. Tech.
Published: 1 February 2016

analysis of CO_2 and $\delta^{13}C$, the size of samples required is large with 800–1000 g but allows measuring a series of other trace gases at the same time (CH_4, CO, and N_2O). The achieved throughput is 3–4 samples per day (Etheridge et al., 1996; MacFarling Meure et al., 2006; Rubino et al., 2013).

In this study, we present a new system built at the Centre for Ice and Climate (CIC, University of Copenhagen, Denmark) in the new laboratory for atmospheric trace gas measurements in ice cores (Stowasser et al., 2012; Sperlich et al., 2013). The approach was to opt for small sample size, allow simultaneous analysis of both CO_2 mixing ratios and its stable isotopic composition on the same sample and to achieve high precision with reasonable throughput in order to pursue high resolution sampling schemes. We thereby followed the extraction principle of the NC using a modified design. Due to the small intended sample size, the extraction unit was coupled to a continuous flow GC–IRMS setup with the benefit of overcoming the problem of interferences from isobaric N_2O and fragments of remaining contamination from drilling liquid.

2 Instrumental setup and standards

2.1 Dry extraction unit

The core of the presented setup is the dry extraction unit. It was designed based on the NC principle for small sample sizes of a few grams described by e.g. Lüthi (2009) and Ahn et al. (2009). However, some major modifications in the design were implemented to achieve the following goals: i) avoiding mechanical friction within the system in order to reduce related contamination and sorption effects (Zumbrunn et al., 1982; Stauffer et al., 1985; Lüthi, 2009), ii) operation at very low temperatures to reduce the risk of CO_2 in situ production (within the extraction unit) from chemical reactions due to the presence of water in the mobile phase and iii) fast and simplified sample loading with minimal exposure of inner surfaces to ambient air in order to maximize sample throughput and to reduce artefacts from surface sorption processes, respectively.

Our design for ice with maximum sample dimensions of 2.3 x 2.5 x 2.5 cm^3 and typical sample mass of 8–13 g is shown in Fig. 1. All inner parts are made from stainless steel (SST). Similar to Ahn et al. (2009), we use a compressible welded bellow (SST, Comvat, Germany, 5 in Fig. 1). This allows crushing of the ice by axial movement of the needles mounted with a

Atmos. Meas. Tech. Discuss., doi:10.5194/amt-2015-351, 2016
Manuscript under review for journal Atmos. Meas. Tech.
Published: 1 February 2016

hot/cold press fit (hardened SST, 1.5 mm O.D., 30 mm length, Dema, Germany, 6 in Fig. 1). Differently from the design described by Lüthi (2009) requiring a vacuum tight seal around a movable piston, no mechanical friction within our unit occurs. Also, the bellow is mounted differently than in the design presented by Ahn et al. (2009) resulting in a 2 times smaller inner volume of 110 cm^3 (63 cm^3 with the bellow compressed) and an inner surface area reduced by a factor of around three. A small volume is favourable in terms of evacuation speed and the time required for transferring the gas out of the extraction unit for subsequent treatment. A small inner surface reduces the potential for surface sorption effects on the CO_2 stable isotope ratios. The extraction unit is connected to the rest of the setup by 1/4 inch SST tubes welded to the NC and equipped with valves (SS–4H, Swagelok, USA, 11, 12 and 13 in Fig. 1). A fixed soft copper seal connects the needle piston to the bellow base plate.

Both the crushing mechanism by axial compression of the bellow and the opening/closing mechanism are pneumatically actuated. To crush the ice sample, a pressure of 4.7 bar is applied to the upper cylinder (CP95SDB40–80, SMC, 1a in Fig. 1) and the needles are actuated via a 5-port solenoid valve (VQZ3120–5YZB–C10, SMC) controlled by an external logical device (homemade). The total number and frequency of strokes can be controlled and were typically set to 37 and ~3 Hz, respectively. Six bar of air pressure applied on the lower actuator (C95NDB80–250, SMC, 1b in Fig. 1) creates enough force for a vacuum tight sealing between the connection of the upper and lower part of the extraction unit using indium wire (1.5 mm OD, 99.99 %, Sigma–Aldrich, USA, 10 in Fig. 1). Although the wire needs to be replaced whenever a new sample is loaded, the Indium can be reused when pressed into wire again. With the sealing mechanism described, screws and their time consuming tightening/untightening are omitted. It takes less than two minutes from opening the device until it is vacuum sealed again, including the removal of the crushed ice, cleaning and loading of a new sample. To minimize contact of ambient air with the inner surfaces and avoid condensation/deposition of water vapour, both the lower and upper part of the device are flushed through the respective inlets with N_2 (99.999 %, Air Liquid, Denmark) whenever the system is opened.

To cool the well-insulated NC, rather than using a liquid cooling fluid, we chose to use an air cooling setup similar to that described in Schmitt (2006). Pressurized air with an adjustable flow between 0 and ~60 L min^{-1} is dried in two sequential traps (filled with Molecular sieve 13X/4A, Supelco, USA) and cooled in a copper heat exchanger mounted in a Dewar (D2). D2 is supplied by droplets of liquid nitrogen (LN) from a larger Dewar (D1) containing the LN

Atmos. Meas. Tech. Discuss., doi:10.5194/amt-2015-351, 2016
Manuscript under review for journal Atmos. Meas. Tech.
Published: 1 February 2016

Atmospheric Measurement Techniques Discussions

reservoir. The droplets are pumped by applying 12.8 V to a heater (10Ω resistor) mounted in the widened inlet of an empty 1/4 inch tube submerged in the LN. Whenever heat is applied, LN evaporates around the heater and the evolving N_2 bubbles transport the still liquid nitrogen above through the isolated tube to D2. This LN pump is regulated by the use of two coupled proportional-integral-derivative controllers (PID, iTRON 08, JUMO, UK). One PID is set to the desired final temperature measured in the NC (9 in Fig. 1) whereas the other is set to a minimum temperature of -180 °C in D2 preventing the system from eventual clogging by frozen rest water in the air stream and potential condensation of oxygen. The temperatures used for PID input and survey of the air stream are measured with platinum resistance thermometers PT100 elements (100 Ω, -200 °C to 600 °C, Class 1/10, TC Direct, USA). By changing the settings for air flow and/or the set points for NC and D2 the air stream temperature is regulated. To cool the NC, the cold air stream is split in front of the unit and either directed through the cavities in the lower part of the massive steel unit (4b in Fig. 1) or the cooling jacket mounted around the compressible welded bellow (4a in Fig. 1). The minimal operating temperature of the NC is -55 °C and standard operating temperature is -45 °C (stability ± 1 °C) with significantly reduced buildup of ice on the vacuum sealing surfaces. While cooling down to -45 °C, the air stream first regulates to about -80 °C before it stabilizes at around -60 °C. Cooling the NC to -45 °C takes around 70 minutes.

Compared to other systems, which operate at -30 °C, the water partial pressure is reduced about 5-fold in our system (-45 °C). Consequently, the risk for wet chemistry in the system producing CO_2 is reduced. This is supported by the findings of Bauska et al. (2014) which indicated that operating at low temperatures improves precision and decreases the blank of the method. Furthermore, the low water vapor partial pressure allowed omitting a water trap at the exit of the extraction unit.

2.2 Analytical system

Our analytical system allows simultaneous measurements of concentrations and stable isotope ratios of atmospheric CO_2 on the same sample. A schematic representation of the system is shown in Fig. 2. It can be divided into two main sections: A) a manually operated section where the standard or sample gas is loaded and B) a fully automated section for gas separation and injection (PreCon) to the detection systems.

Section A consists of four main parts:

(i) a vacuum line,

Atmos. Meas. Tech. Discuss., doi:10.5194/amt-2015-351, 2016
Manuscript under review for journal Atmos. Meas. Tech.
Published: 1 February 2016

(ii) a gas manifold for carrier-, protection- or standard-gas injection,
(iii) a dry extraction unit and
(iv) a trap (T1) to quantitatively cryopump sampled gas out of the extraction unit for subsequent and complete transfer from section A to B.

Section B consists of two main parts:
(i) a gas chromatography setup which allows trapping the transferred gas sample (T2), separation of CO_2 (and N_2O) from the major air components (T3) and subsequent partitioning of the two fractions to individual lines for either final detection or further purification (GC–1), focusing (CF) and CO_2/N_2O separation (GC–2),
(ii) the detection systems including a thermal conductivity detector (TCD, VICI, USA, integral part of GC–1, TRACE GC Ultra, Thermo Scientific, USA) to quantify the amount of the main air fraction, a pulsed discharge detector (PDD, VICI, USA, integral part of GC–1) to survey CO_2 separation and purification and an IRMS (Delta V Plus, Thermo Fisher, Germany) to quantify the amount and stable isotope ratios of the CO_2 fraction.

All inner surfaces of the setup are either made from SST or fused silica and the connections are either welded or sealed with metal or graphite/vespel ferrules to exclude artefacts due to out-gassing (Sturm et al., 2004). Section A can either be evacuated or flushed with N_2 (inert gas also used for protection of inner surfaces when the extraction unit is opened) or He (99.9995 %, Air Liquide, Denmark) additionally purified by a getter (Gas Purifier, VICI, Valco Instruments Co. Inc, USA). Similar to the gas manifold, the vacuum line is made from 1/4 inch SST tubes and equipped with on/off valves (SS–4H, Swagelok, USA). It includes a low vacuum (LV) rotary vane pump (Edwards, EDM2) and a turbo pump (TMU 071, Pfeiffer, Germany) to reach high vacuum (HV). The LV pump is used for fast removal of large quantities of gas (i.e. after sample loading) and is protected from the analytical line by a liquid nitrogen trap (WT). All lines in section B are always above atmospheric pressure and continuously flushed with He used as carrier gas for the entire system, allowing transfer of sample/standard gas from the extraction unit to the detection systems which are all run in continuous flow mode. Further details will be given in Chapter 3.

2.3 Standards

CO_2 concentrations are reported in parts per million (ppm) and are referenced to the World Meteorological Organization (WMO) mole fraction scale for CO_2 in air (Tans and Zhao,

Atmos. Meas. Tech. Discuss., doi:10.5194/amt-2015-351, 2016
Manuscript under review for journal Atmos. Meas. Tech.
Published: 1 February 2016

Atmospheric Measurement Techniques Discussions

2003; Zhao and Tans, 2006). Isotope ratios (R) are reported using the delta (δ) notation and are referenced to the respective international isotope scale (VPDB and VPDB-CO_2 for δ^{13}C-CO_2 and δ^{18}O-CO_2) as described by the following equation:

$$\delta^m E_{sample/reference} = \left[\frac{Rm(sample) - Rm(reference)}{Rm(reference)} \right] \quad (1)$$

where *m* designates the rare isotope of element E (e.g., m = 13 for $^{13}C/^{12}C$, or m = 18 for $^{18}O/^{16}O$). For reporting purposes the delta value is multiplied by 1000, which is denoted by the symbol per mill (‰). The range of our standards was selected in order to cover the expected atmospheric concentration and stable isotopic composition values for glacial to interglacial conditions (Table 1). With these standards, system characterisation, daily calibration and continuous quality control sample measurements (QCS) were performed (see Chapter 3 and 4).

For referencing IRMS measurements, a working standard (WS) of pure CO_2 from a natural source (Messer–649250, Messer, Italy) is injected via an open-split interface (GC interface). Its stable isotopic composition was referenced at CIC via IRMS Dual Inlet measurements (Delta V Plus, Thermo Fisher, Germany) against pure CO_2 reference gases GS19 and GS20 from the Centre for Isotope Research, Gröningen University, Netherlands (Meijer, 1995). For air standards we used three synthetic air mixtures, in the following called CA08274, CA08054 and CA08292 and provided by the Global Monitoring Division of the Earth System Research Laboratory at the National Oceanic and Atmospheric Administration (NOAA ESRL/GMD, Boulder, USA), two pressurized air tanks called AL–1 and AL–2 (Air Liquid, Denmark) and one of two atmospheric air tanks sampled in 2008 at a clean-air site of the NEEM deep ice core drilling camp called NEEM–2. For the three NOAA tanks, CO_2 concentrations have been calibrated and certified by the NOAA Carbon Cycle Gases Group of the Global Monitoring Division. The other tanks have been calibrated at CIC against these three standards both with the setup described in this study and a laser spectrometer (Picarro Inc., USA). The stable isotopic composition of CA08054 has been calibrated by the Stable Isotope Lab at INSTAAR (SIOL, University of Colorado) in cooperation with the NOAA Climate Monitoring and Diagnostics division (CMDL). For the other two NOAA cylinders, AL–1, AL–2 and NEEM–2 the stable isotopic composition has been calibrated at CIC against Messer–649250 and CA08054 also with the setup described here. All tanks were equipped

Atmos. Meas. Tech. Discuss., doi:10.5194/amt-2015-351, 2016
Manuscript under review for journal Atmos. Meas. Tech.
Published: 1 February 2016

with high purity regulators (Y13–C444A, single stage, stainless steel with Kel–F and Teflon seals, Airgas, USA).

3 Measurement procedures and quality control

3.1 PreCon system

As mentioned in Sect. 2.3, the pure CO_2-WS (Messer–649250) is injected via an open-split interface (GC interface) for referencing of IRMS measurements. The WS can optionally also be passed through the automated section B of the system (see Fig. 2). This allows the assessment of potential fractionation effects from gas trapping and GC separation (see Chapter 4). In the daily routine it is useful for an immediate control of conditions and stability of the pre-concentration, gas chromatography and detection systems. Such injections, variable in the amount, were therefore performed at the beginning of each measurement day together with blank runs for this part of the setup (Table 2).

In detail, various amounts of pure CO_2-WS are injected directly onto the cryogenic trap T2 (1/4 inch SST Swagelok tube, filled with around 5 cm of HayeSep D, 100/120 mesh, Sigma–Aldrich, Switzerland) with valve V1 (10-port, 1/8 inch, air actuated, A210UWM, VICI, USA) switched compared to Fig. 2. T2 is previously cooled by immersing into liquid nitrogen with V1 in the initial position. Another trap T3 (empty 1/16 inch SST Swagelok tube connected in series with T2) is cooled down simultaneously. In order to prevent ambient air to be sucked into T2 and T3 while cooling down, the on/off valve (SS–4BK–TW–1C, Swagelok, USA) at the vent is closed. To vary the injected amount of the reference CO_2 (i.e. WS) an internal sample injection valve with a defined volume of 0.1 µl (injV, AN14WM.1, VICI, USA) is switched by the selected number of times. Alternatively, if the valve is not switched, a blank measurement for this section of the system is obtained since only Helium carrier gas is passed through the system (20 ml min^{-1}, set by a flow controller, Model VCD 1000, Porter, USA). In any case, V2 (6-port, 5UWM, VICI, USA) is switched after a trapping time of six minutes – similar to the trapping time applied for air standard and ice sample measurements – directing the sample gas flow (10 ml min^{-1} set by a flow controller; VCD 1000, Porter, USA) through the TCD detector. After an idle time of 30s allowing the flow to stabilize, the LN Dewar cooling T2 and T3 is automatically lowered by a double activated pneumatic cylinder (CD85N20–250B, SMC, Denmark) to a level at which T3 is still cooled.

Atmos. Meas. Tech. Discuss., doi:10.5194/amt-2015-351, 2016
Manuscript under review for journal Atmos. Meas. Tech.
Published: 1 February 2016

Atmospheric Measurement Techniques Discussions

T2 is then heated by a rope heater (FGR–060, Omegalux, UK) to the set temperature of 150 °C regulated by a PID controller (iTRON 08, JUMO, UK). Thereby, the trapped gas is released and the amount of the main air components is detected by the TCD (no signal detected here for the pure CO_2 and blank measurements) while both CO_2 and N_2O are subsequently trapped in T3 for later separation and analysis by the PDD and IRMS in a second detection line. Typical chromatograms from the TCD, PDD and IRMS for the measurement of the pure CO_2-WS can be found in the Supplement (Fig. S1). After 5 minutes, V2 is switched again, redirecting the sample flow (again 20 ml min^{-1}) through the alternative detection line. After an idle time of 40 s allowing the flow to stabilize, the LN Dewar is further lowered and trap T3 quickly heated to 100 °C (resistance wire, 2.5 Ω m^{-1}, 5 m, Conrad Electronics, Germany) regulated by a second PID controller (iTRON 32, JUMO, UK). Thereby, CO_2 and N_2O (not present in the pure CO_2-WS) are released and the different gases subsequently chromatographically separated by the gas chromatographic fused silica capillary column in the GC–1 (30°C, CP–PoraBond–Q, 25 m x 0.53 mm, df = 10µm, Varian, USA) before being detected by the PDD (discharge gas flow set to 30 ml min^{-1}) shown in Fig. S1. Shortly before the eluted CO_2 peak arrives at the PDD, three parallel traps (fused silica capillaries, 250 µm ID, 1.8 m length, BGB, Germany) split the sample stream after V3 at the PDD outlet (GC built in 6-port valve, VICI, USA) and are immersed into LN to retrap CO_2 and N_2O for cryogenic focus (CF). To vent remaining H_2O and potential contaminants from drilling fluid (primarily/exclusively present in samples extracted from ice) V3 is switched before signal detection in the PDD (~70 s after the maximum in the CO_2 peak) and the GC column is heated to 150 °C. In parallel, the three CF capillaries are lifted one after the other out of the LN, subsequently releasing the sample – now split in three aliquots – for further transport in a reduced He flow of 1.5 ml min^{-1}. CO_2 and N_2O contained in these aliquots are again separated by the GC column in GC–2 (35°C, CP–PoraBond–Q, 40 cm x 0.53 mm, df = 10µm, Varian, USA) and remnant water vapour is removed by a Nafion drying column (0.36 mm I.D. x 40 cm, Perma Pure Inc., USA). Finally, the sample gases are introduced to the IRMS via the GC interface. Before the three CO_2 sample peaks elute, multiple injections of the CO_2-WS (in this case the same gas as the sample gas) with the amplitude of the on/off peaks closely matching the size of the sample (not for blanks) are performed in order to reach stable IRMS-source conditions (Fig. S1). For the same reason a constant CO background flow through the reference open split port into the ion source was maintained as proposed in

Atmos. Meas. Tech. Discuss., doi:10.5194/amt-2015-351, 2016
Manuscript under review for journal Atmos. Meas. Tech.
Published: 1 February 2016

Elsig and Leuenberger (2010). The mean value of the peak before and after the sample is finally used for referencing (see Fig. 2).

The total measurement time from injection to final IRMS detection is 21 minutes. It is longer for air standard and ice sample measurements also including section A of the system (Sect. 3.2).

3.2 Standard air, ice samples and blanks

Air standards and blank measurements were performed regularly for calibration and system characterisation thereby following the exact procedure used to measure real (natural) ice samples, i.e. following the 'Identical Treatment' principle (Werner and Brand, 2001). To simulate the entire measurement procedure as close as possible, artificial bubble free ice samples (BFI) were used. BFI was produced from ultrapure water (MilliQ,18.2 MΩ cm at 25 °C) degassed for 60–90 minutes using a roughing LV pump (E2M0.7, Edwards, UK) and then slowly frozen from the bottom (20 cm in 48 hours) thereby forcing the remaining gas out of the water prior to freezing. Results for calibrations and system characterisation will be presented in Chapter 4.

Samples of air, either from pressurized flasks/cylinders (e.g. atmospheric samples or standards) or extracted from ice core samples require and pass all sections of the experimental setup (A and B, Fig. 2). When the system is not in use (e.g. overnight), section B is constantly flushed with He while all lines in section A and the NC are pressurized slightly above atmospheric pressure with He and N_2, respectively. Prior to analysis, ice core or BFI samples are cut to the required dimensions and surfaces decontaminated by chiselling off the top layers with a scalpel.

A typical daily measurement sequence with alternative options indicated in addition is listed in Table 2. The measurements can be distinguished in five main categories: 1) Standard measurements performed by injecting the standard gas over an ice sample of either natural or artificial origin (BFI) without crushing the ice. Used standards were different in their CO_2 mixing ratio and isotopic composition (Table 1) and the introduced amount of gas was varied. 2) System blank measurements performed by omitting addition of standard gas and hence resulting in sampling carrier gas only (see chromatogram in Fig. S2). 3) BFI measurements either performed with air standard added or omitted but with the ice being crushed. 4) Measurements performed after (3), again moving the needles but using the already crushed

Atmos. Meas. Tech. Discuss., doi:10.5194/amt-2015-351, 2016
Manuscript under review for journal Atmos. Meas. Tech.
Published: 1 February 2016

Atmospheric Measurement Techniques Discussions

ice. This closely simulates the crushing step and the associated effects. Artefacts due to remnant gas potentially present in the initial (i.e. uncrushed) BFI analyzed in (3) can however be excluded (see Chapter 4). These measurements were also performed with and without the addition of air standard. The latter case will in the following be referred to as "procedural blank". 5) At last, measurements of air extracted from natural ice samples by crushing the ice.

In the following we give a step by step description of the measurement procedure. Section A and the NC are prepared for measurements during the first five runs of the daily sequence (Table 2). The procedure for these runs is described in Sect. 3.1. After the air cooling system of the NC is started, the first ice sample is loaded once a temperature of -20 °C has been reached. While the unit is open, both the upper and lower part are continuously flushed with N_2 through the respective inlets (11 and 12 in Fig. 1 and 2) to prevent contamination from ambient air and condensation of water vapour on the cold inner surfaces. After the NC is closed and vacuum sealed again, inlets 11 and 12 are closed and the N_2 flow turned off. Each time the NC has been opened, the following sequence of steps is required for evacuation and reconditioning. The chamber is evacuated by the LV pump through inlet 11 for one minute. Only port 11 is used in this evacuation step to prevent trapping of N_2 on trap T1 (heated to 100ºC, 1/4 inch SST tube, filled with HayeSep D, 100/120 mesh, Sigma–Aldrich). This is essential because at this point the N_2 abundance in the NC is much higher than in samples of recent or past atmosphere. Inlet 12, mounted at the bottom part remains always closed when the system is evacuated. To avoid analytical artefacts, this inlet is only used with a one directional flow into the NC to prevent water vapour from reaching the gas manifold and the vacuum lines used for the injection of standard air samples. When the pressure in the NC has dropped, trap T1 and the rest of the vacuum lines still filled with He or N_2, respectively, are now also evacuated through their respective evacuation lines. After a few seconds the vacuum system is switched to the HV pump for another five minutes. To precondition the NC, the chamber is closed off towards vacuum by closing inlet 11 and outlet 13 (Fig. 1 and 2). Then it is filled with an aliquot of air standard, expanded from the gas manifold, through inlet 12. Since in this step the standard addition is only for reconditioning, it is not done in a quantitative way. After inlet 12 is closed again, T1 is cooled down being immersed in LN before outlet 13 is opened in order to cryogenically pump the air aliquot on T1. After a three minute trapping time, the line (vacuum line–NC–T1) is flushed with He from the inlet next to the gas manifold set to a flow of 80 ml min^{-1} (gas flow controller, Model 100, VICI, USA). Since this air aliquot is not to be analyzed, the He gas flow is thereby directed through the 3

Atmos. Meas. Tech. Discuss., doi:10.5194/amt-2015-351, 2016
Manuscript under review for journal Atmos. Meas. Tech.
Published: 1 February 2016

way valve (3–WV in Fig. 2, SS–43GXS4, Swagelok, USA) into the LV pump. To release the previously trapped air sample while flushing, T1 is heated by a rope heater (FGR–060, Omegalux, UK) to the set temperature of 150 °C regulated by a PID controller (N2300, West Instruments, USA). After a flushing time of three minutes, outlet 13 and inlet 12 are closed and the temperature of T1 is reduced to 100 °C again. The system is now in a similar state as it would be prior to runs where the NC has not been opened beforehand (see Table 2).

To start an acquisition run, the NC, T1 and all vacuum lines are evacuated for ~10 minutes until reaching a pressure of $2x10^{-3}$ mbar monitored by P1 (Single Gauge Pirani Transmitter, Pfeiffer, Germany; in a dry system, a vacuum < $5x10^{-4}$ mbar, the lower limit of P1 is reached). The gas manifold allows selection between the different air standards (denoted as STD in Fig. 2) and the amount to be injected. For this purpose, gas can be expanded into a defined volume adjustable in size by the valves included in each line. For each expansion step an equilibrium time of two minutes was applied. The first run in the sequence including section A is always an air standard of large size (run 6), i.e. a standard aliquot expanded from the volume between the first and last valve of the gas manifold line. This allows for a first immediate control of the day by day system stability and conditions the entire system with an air sample after the idle time overnight. From the gas manifold the sample is expanded into a defined volume of ~11 cm^3 (DF, Fig. 2) equipped with another pressure gauge P2 (high precision piezo pressure transmitter, PAA–35X, Keller AG, Switzerland). After DF has been closed off (with the valve at inlet 12 already being closed beforehand) the pressure is recorded for later use (see Sect. 4.1.1). At the same time, sample air contained in the rest of the lines is pumped off by the HV pump. After the pressure reading has been performed, the gas is further expanded into the NC disconnected from the vacuum beforehand. The air standard sample is kept in the NC for two minutes, simulating the procedure applied for natural ice samples which are crushed at this point and gas is allowed to subsequently expand from the ice. The valve to DF is thereby kept open, which on the one hand allows to record and survey the efficiency of gas extraction from the opened bubbles when measuring natural ice samples and on the other hand the gas transfer out of the NC onto the precooled trap T1 in the following three minute cryogenic pumping step. Afterwards, with the cryopump still active (i.e. T1 still cooled with LN), the NC and T1 are filled with He (80 ml min^{-1}) to 1100 mbar which is slightly above the pressure in section B (~3 min). This prevents back flushing from section B to A when they are then connected by switching the 3–WV. Now, the air sample is released by heating T1 to the set temperature of 150 °C and transferred to the

Atmos. Meas. Tech. Discuss., doi:10.5194/amt-2015-351, 2016
Manuscript under review for journal Atmos. Meas. Tech.
Published: 1 February 2016

precooled trap T2 by the carrier gas (80 ml min^{-1}). This step takes another three minutes. The 3–WV is then closed, again separating section A and B. From here on, the sample is in a reduced carrier gas flow environment and treated precisely as described in Sect. 3.1 while section A can be prepared for the next sample. Therefore, the outlet valve of the NC is closed, the N_2 flush flow opened and the next ice cube loaded. In case the next sample in the sequence (Table 2) is measured with the ice remaining in the NC, the extraction unit and the vacuum lines are evacuated to prepare for the next run.

For the measurement of natural ice samples, the procedure is as described above but skipping the addition of air standard. Chromatograms of the TCD, PDD and IRMS for a typical ice sample measurement are shown in Fig. 3. Here, opposed to measurements of pure CO_2-WS (Sect. 3.1, Fig. S1) and blanks (e.g. Fig. S2), the peak from sample air shows up as a distinct TCD signal and signals of H_2O from ice sample water vapor and remnants of drilling liquid contamination are detected by the PDD.

A number of additional steps are necessary compared to the measurements described in Sect. 3.1. However, the procedure described here, does not take much longer because once the sample has been transferred from T1 to T2, section A can be prepared for the next sample while the current measurement is simultaneously running in section B. Typically, the analysis takes around 30 minutes (run to run). Obviously it increases for runs requiring loading of a new ice sample and thus the opening of the NC followed by additional evacuation and flushing steps (~50 min, e.g. runs 6, 11, 14 and 18 in Table 2).

4 Results and discussion

4.1 Evaluation and calibration

System-specific analytical bias for CO_2 concentration and stable isotope measurements can result from various fractionation processes in the analytical system such as sorption effects, specifically in the extraction unit (Zumbrunn et al., 1982), non-quantitative trapping and releasing of gas and from GC separation. For stable isotope measurements, further bias arises from IRMS injection and source effects (Elsig and Leuenberger, 2010). The net effect of these processes was assessed and monitored on a regular basis to account for system drifts. Such drifts may occur when boundary conditions (e.g. room temperature) change and can occur within a measurement day, on a day to day basis and on longer time scales where they

Atmos. Meas. Tech. Discuss., doi:10.5194/amt-2015-351, 2016
Manuscript under review for journal Atmos. Meas. Tech.
Published: 1 February 2016

might be related to changes in the setup (e.g. replacements of parts, change of carrier gas tanks or standards, adjustments in carrier gas flows or small improvements in the procedure). Following the 'Identical Treatment' principle (Werner and Brand, 2001) we characterized all sections of our system for systematic effects using the various standards available (Table 1) allowing a reliable correction of the raw data. Runs of quality control samples (QCS) to assess long-term stability of our final measurement results were carried out on a daily basis (for results see Sect. 4.2.1).

4.1.1 CO_2

CO_2 concentrations can in principle be derived from the ratio between the IRMS CO_2 peak area (values given in the following always denote the mean for the three sample peaks) and the major air components detected as TCD peak area (Fig. 3). The TCD air peak signal was observed to be nonlinearly related to the amount of air with significant variability. This can be seen in the relation between the high precision pressure readings of standard gas (described in Sect. 3.2.) and the TCD air peak area investigated for different measurement periods (Fig. 4A). We also found variability in the relation between the IRMS peak area and the CO_2 amount; in this case, however, the relationship is linear. Reasons for the observed variability are manifold; e.g. small adjustments in flow, trapping procedures or small changes in outer conditions such as room temperature (e.g. March and June 2012).

To avoid nonlinearity in data processing, the TCD signal was converted to pressure using the second order polynomial functions shown in Fig. 4A. The functions can be determined for any user-defined period of time with the data obtained from daily performed measurements of air standards. In doing so, the large long-term variations in TCD sensitivity are accounted for and all TCD measurements adjusted and referred to a common scale (pressure). CO_2 concentrations were then related to the ratio between the IRMS CO_2 peak area and the computed pressure. By including data of all available standards, the resulting linear calibration curve is well defined over a large concentration range (Fig. 4B). The data shown is based on repeated measurements series over the course of more than one year (n = 4). Each series was performed on a single day with the entire range of standards being measured at least 3 times. The ratios calculated for the individual series were matched for CA08054 in order to account for the long term variation of the IRMS response, resulting in the shown average transfer function.

Atmos. Meas. Tech. Discuss., doi:10.5194/amt-2015-351, 2016
Manuscript under review for journal Atmos. Meas. Tech.
Published: 1 February 2016

Atmospheric Measurement Techniques Discussions

With the calibration curve covering the entire range of expected measurement results (Fig. 4B), daily calibration could be performed with a subset of standards only, thus significantly reducing the total sequence time. Summarized in Table 2, a typical daily measurement sequence includes the repeated measurement of standard CA08504 (run 8, 10, 13 and 20) to determine and subsequently adjust for i) potential offset in the calculated ratio compared to the calibration curve and ii) system drift over the sequence measurement time. It further includes at least one additional standard gas measurement with a different CO_2 mixing ratio to adjust for variations in the slope of the linear calibration fit (run 16, 21 and 17 if necessary). If not used in the daily calibration, run 17 is treated similarly to a real sample in the post processing of the raw data, allowing us to assess the long term consistency and precision of our measurements (QCS, see Sect. 4.2.1). In run 21, CA08504 is occasionally injected in variable amounts to ensure the independency of final results from sampled amount of gas.

We find that independent of sample size, gas amount, or concentration, a constant amount of CO_2 is produced by the extraction itself. This amount was determined by measurements of BFI samples. To perfectly simulate measurements of natural ice samples according to the 'Identical Treatment' principle (Werner and Brand, 2001), artificially produced bubble ice with entrapped standard gases would be required. Because this is technically not feasible, we instead added standard gas to a BFI sample loaded in the NC and crushed for the measurement. The CO_2 mixing ratios we observed were elevated by 4.6 ± 2.6 ppm on average (n = 5) compared to the expected value. However, for subsequent measurements with identical procedure (including movement of needle pins) but using the previously crushed BFI the elevation was only 2.3 ± 2.0 ppm on average (n = 5). We considered this lower value to be more representative for the system related effects because small amounts of remnant gases in our BFI are very likely. In any case, the CO_2 enrichment – expressed in ppm before – is detected in the raw data as an elevated signal in the IRMS CO_2 peak area. This surplus signal can also reliably be obtained from the measurement of a procedural blank following the exact same procedure as described above, using already crushed BFI (see Fig. S3). This is a more straightforward and beneficial approach because air standard addition can be omitted and data post-processing with the associated propagation of uncertainties is significantly reduced. Combining the results from both approaches, the IRMS CO_2 peak area for the procedural blank was observed to be 0.5 ± 0.2 mVs on average (n = 9), i.e. elevated by 0.1 ±

Atmos. Meas. Tech. Discuss., doi:10.5194/amt-2015-351, 2016
Manuscript under review for journal Atmos. Meas. Tech.
Published: 1 February 2016

Atmospheric Measurement Techniques Discussions

0.1 mVs compared to the system blank (see Sect. 4.1.2). The finally applied procedural blank correction will be described and discussed in Sect. 4.1.3.

4.1.2 $\delta^{13}C$-CO_2 and $\delta^{18}O$-CO_2

Individual sections of the setup were characterized for systematic effects on $\delta^{13}C$ and $\delta^{18}O$ results. Calibrations, control of system stability and blanks as well as QCS measurements to assure the long term quality of our analysis (Sect. 4.2.1) were all performed on a daily basis (Table 2).

We characterized the IRMS source effects – in the following denoted as IRMS nonlinearity – by measurements of reference gas (CO_2-WS) injected via the reference open split (Fig. 2). To reach stable source conditions, six injections were made prior to acquisition similar to the approach described in Elsig and Leuenberger (2010). Then, the injection amount was step-wise increased, reflected in rising amplitudes of the rectangular peaks. The signal amplitude (mass 44) thereby ranged between 400 and 8400 mV with the reference peak always set to around 4000 mV (gain: R = 10^8 Ω). This experiment was replicated on three different days distributed over a time period of one year. The resulting total number of acquisitions was 177. In Fig. 5A, the IRMS nonlinearity effect for $\delta^{13}C$ is shown, measured as the deviation from the reference (~4000 mV). In the supplementary material, the equivalent figure can be found for $\delta^{18}O$ (Fig. S3).

To assess the relation between sample amount and the stable isotope values for the automated section B of the setup (Fig. 2) – in the following referred to as pre-concentration and GC effect (PreCon–GC effect) – various amounts of the WS used for the IRMS nonlinearity test were injected onto trap T2 via the VICI injection valve with an internal volume of 0.1 µl (injV, Fig. 2). The idea is to cover all potential effects related to trapping and releasing of CO_2 on traps T2, T3, the gas chromatographic separation in GC–1 and GC–2, cryofocusing (CF), the injection via the sample open split and any effects related to sorption processes in the lines. For this part of the setup, blanks were analyzed in addition. Therefore injection of CO_2 was omitted but otherwise the exact same procedure was followed (see Sect. 3.1). To separate the effect specific to this part of the section (B) from the other effects involved, the obtained raw data was first corrected for the IRMS nonlinearity by applying the third order polynomial fit shown in Fig. 5A and the blank contribution characterized for this part of the setup. To correct for the blank, the following equation to calculate in close approximation the

Atmos. Meas. Tech. Discuss., doi:10.5194/amt-2015-351, 2016
Manuscript under review for journal Atmos. Meas. Tech.
Published: 1 February 2016

isotopic abundance in a pool derived by the combination of isotopically different materials was accordingly reformulated:

$$\delta_{\Sigma} = \frac{\Sigma m_i \delta_i}{\Sigma m_i} \quad (2)$$

Eq. (2) shows that the bigger the CO_2 blank to sample ratio and the difference between blank and sample isotopic composition, the bigger the blank correction will be. In other words, even if the blank is constant both in size and isotopic composition, the size of the blank correction will vary dependent on both, the CO_2 mixing ratio and the isotopic composition of the sample analyzed but also on the sampled amount of air. Due to the large number of variables involved, it is obviously important to carefully disentangle blank related from other system induced effects influencing the observed isotopic signal. After blank correction based on Eq. (2), the PreCon–GC effect determined can be applied for the correction of all types of samples, independent of their characteristics, at least in a first order approximation. A potential effect related to the gas matrix, i.e. the presence of major air components in the sample will be discussed below. Shown in Fig. 5B is the finally derived linear relationship for the PreCon–GC section. In the supplementary material, the equivalent figure can be found for $\delta^{18}O$ (Fig. S3). It needs to be noted that the isotopic values of the blanks are affected similarly to any other sample by systematic effects including the IRMS nonlinearity but also the PreCon–GC effect investigated here. Therefore, the final relationship shown in Fig. 5B and the values used for the blank correction were derived iteratively (n = 5; i.e. until changes were well below IRMS precision). Final mean values for blanks (n = 99) were reproducible for the acquired two year time period with 0.09 ± 0.02 mVs, -24.2 ± 1.9 ‰ and -41 ± 5 ‰ for CO_2 IRMS peak area, $\delta^{13}C$ and $\delta^{18}O$, respectively. This reveals the blank isotopic values to be heavily depleted compared to atmospheric values. This is consistent with the idea of a constant release of tiny amounts from CO_2 absorbed to e.g. system surfaces, trapping material and GC columns, resulting in heavy fractionation. To test if the measured isotopic values are reliable although measured on extremely small sample amounts, comparable amounts of CO_2-WS were directly injected via the sample open split resulting in a similar peak shape (n = 5, IRMS peak area between 0.14 and 1.17 mVs). After correction for the IRMS nonlinearity effect, we obtained average values of -6.5 ± 0.6 ‰ and -11.7 ± 1.6 ‰ for $\delta^{13}C$ and $\delta^{18}O$, respectively. They are not significantly different from the "true" value of the WS (-6.004 ± 0.008 ‰ and -10.80 ± 0.13 ‰), thus demonstrating the reliability of measurements

Atmos. Meas. Tech. Discuss., doi:10.5194/amt-2015-351, 2016
Manuscript under review for journal Atmos. Meas. Tech.
Published: 1 February 2016

even for very small sample amounts and adding confidence in the determined values for the blank.

To investigate the characteristic of section A of the system and a potential gas matrix effect (i.e. a different behaviour of CO_2 as a trace gas in air) happening in the PreCon–GC section discussed above, the CA08054 air standard was analyzed over ice in variable gas amounts (see Sect. 3.2. for methodology). In the following, this will be denoted as the "air amount dependence". In repeated series (n = 10), distributed over a time period of more than one year, 46 such measurements were made. In addition, 42 blanks (omitting sample injection but exactly following the procedure otherwise) were measured. Following the approach for determination of the PreCon–GC linearity, the blank contribution was separated from the effect investigated here. Again, measured isotopic values of the blank finally used for blank correction first needed to be corrected for the investigated effects like all other samples. Consequently, corrections for IRMS nonlinearity, PreCon–GC linearity and the air amount dependence discussed here (derived by iteration) were applied. The blank value obtained here, representative of the entire setup and accordingly denoted as "system blank", was 0.4 ± 0.1 mVs, -27.6 ± 1.2 ‰ and -30 ± 3 ‰ for CO_2 peak area, $\delta^{13}C$ and $\delta^{18}O$, respectively. Because of the large additional surface area from extra lines and the NC chamber and one additional trap (T1), the system blank is bigger in size than the blank observed for the PreCon–GC section alone (see above). However, the obtained values for their isotopic composition are comparable. This again adds confidence into these depleted values because it indicates the responsible fractionation effects, most likely caused by sorption processes, to be similar in the different sections of the setup in agreement to expectations due to the similarity of the built-in parts. The final relationship for the air amount dependence is presented in Fig. 5C was obtained after correction for IRMS nonlinearity, PreCon–GC linearity and the blank contribution just described. In the supplementary material, the equivalent figure can be found for $\delta^{18}O$ (Fig. S3).

To fulfill the "Identical Treatment" principle, the crushing step was included to assess the procedural blank of ice sample measurements. The procedural blank amounts to 0.5 ± 0.2 mVs in the CO_2 IRMS peak area (Sect. 4.1.1). Neglecting the effect from the remnant gas in the BFI , the results from standard measurements while crushing the BFI and the consecutive ones with the pins also being moved but using the previously crushed ice as described in Sect. 4.1.1 were combined to determine the difference between measured and expected $\delta^{13}C$ values. Reformulating Eq. (2) then allowed calculating the isotopic composition of the

Atmos. Meas. Tech. Discuss., doi:10.5194/amt-2015-351, 2016
Manuscript under review for journal Atmos. Meas. Tech.
Published: 1 February 2016

procedural blank since the total amount of gas, the amount of the blank, the isotopic composition of the standard and the isotopic composition of the gas total is known. This results in a value of -24 ± 3 ‰ and -28 ± 4 ‰ for $\delta^{13}C$ and $\delta^{18}O$, respectively. This approach to determine the isotopic value of the procedural blank relies on the measurement of normal size gas samples due to the standard gas added. However, within uncertainties, the results are consistent with the direct measurement of the isotopic composition of the procedural blank (no standard added, pins moved and using previously crushed BFI) resulting in a value of -26.6 ± 0.8 ‰ and -29 ± 3 ‰ for $\delta^{13}C$ and $\delta^{18}O$, respectively (n=4). This reconfirms the reliability of our blank measurements although performed on extremely small sample amounts and further verifies the found heavily depleted isotopic composition. The finally applied procedural blank correction will be described and discussed in Sect. 4.1.3.

To account for the effects characterized in this Section, post-processing of raw data involved correction in the given order for: 1) IRMS nonlinearity, 2) PreCon–GC linearity, 3) air amount dependence linearity and 4) blank contribution. The repeated measurement of air standards varying in concentration and isotopic composition (runs 8, 10, 13, 16, 20, 21 and 17 in some cases) were then used for daily calibration to adjust for potential day by day offsets and daily drift. If not used for calibration, run 17 was treated as a QCS (see Sect. 4.2.1). In run 21, CA08504 is occasionally injected in variable amounts to further ensure the independence of final results from sample gas amount. Results and achieved precision for the measurements of ice samples will be discussed in Sect. 4.2.2.

4.1.3 Procedural blank correction

A thorough understanding of the blank and its effect on the analytical results of CO_2 and $\delta^{13}C$ is crucial. The system blank is considered for the analysis of standard air samples used for calibration of the results. However, the procedural blank relevant for the measurement of ice core samples includes additional CO_2 contribution from processes not covered by the system blank (e.g. sample preparation or mechanical movement in the NC). In the literature, the common approach to account (i.e. correct) for this surplus procedural blank contribution is to finally subtract a constant offset for the ice core sample CO_2 mixing and isotopes ratio results (e.g. Elsig et al., 2009; Schmitt et al., 2011; Rubino et al., 2013). In this study, the offset value for CO_2 measurements would correspond to the 2.3 ± 2.0 ppm determined in Sect. 4.1.1. However, this approach implies the assumption of a surplus CO_2 procedural blank contribution which is variable in terms of amount (i.e. moles), for all samples coincidentally

Atmos. Meas. Tech. Discuss., doi:10.5194/amt-2015-351, 2016
Manuscript under review for journal Atmos. Meas. Tech.
Published: 1 February 2016

resulting in the exact same offset in terms of ppm, independent of their CO_2 mixing ratio and the extracted amount of air. As this is unlikely to occur, a compressed scale for data covering a large range of concentrations needs to be expected (e.g. Glacial–Interglacial atmospheric conditions ranging from around 180 ppm to the current atmospheric level of almost 400 ppm). Whereas for measurements with large sample sizes, i.e. low blank to sample ratios, this bias might be negligible considering analytical uncertainties, a different, more accurate correction of the procedural blank should be applied for measurements using small samples. In this study, we therefore assumed constant surplus CO_2 contribution in terms of amount instead of concentration (i.e. moles not ppm), which is in agreement with our observations. Accordingly, we subtracted the additional CO_2 contribution expressed in surplus IRMS CO_2 peak area from the raw data prior to conversion into ppm. For the small sample sizes analyzed in this study, the improvement of this new approach is directly reflected in a reduced standard deviation obtained for the results from sets of replicate measurements of ice from the same site and sampling depth but slightly differing in the sampled gas amount (see Sect. 4.2.2). For these samples, the applied correction varied between 1.9 and 3.3 ppm (2.4 ppm on average, n = 18).

For the procedural blank correction of isotopic values the common approach to subtract a constant offset is even more critical. As discussed in Sect. 4.1.2 – even for blanks constant in CO_2 contribution and isotopic composition – the size of the procedural blank correction should be dependent on the size, CO_2 mixing ratio and the isotopic composition of the sample analyzed. Obviously, the bigger the CO_2 blank to sample ratio and the difference between blank and sample isotopic composition, the bigger the correction will be. Considering the observed, heavily depleted isotopic composition of the blank CO_2 (Sect. 4.1.2) the variation of the correction might be significant even for samples of larger size. For sample sizes 10 times bigger than the ones analyzed in this study (i.e. ~100 g ice) and employing Eq. (2), the scale compression bias resulting from the application of the conventional approach was calculated for an ice core record covering the Holocene (approximated range: 370 to 180 ppm in CO_2 and -6.6 to -6.3 ‰ in $\delta^{13}C$) if considering the observed low value of -27.6 ‰ for the isotopic composition of the blank. Further, we assumed procedural blanks of 1 ppm CO_2 and 0.1 ‰ $\delta^{13}C$ which are typical literature values and smaller compared to the numbers determined in this study. The calculation does not consider a potential additional effect arising from variations in ice sample size used to obtain the record. With these numbers, the expected scale compression bias arising from the commonly applied procedural blank

Atmos. Meas. Tech. Discuss., doi:10.5194/amt-2015-351, 2016
Manuscript under review for journal Atmos. Meas. Tech.
Published: 1 February 2016

correction is calculated to be 0.06 ‰. This demonstrates that even for larger sample sizes this bias is significant considering the recent improvements in analytical precision. Obviously, it becomes particularly important for higher blank to sample ratios (e.g. small sample sizes). Here we thus applied a new, more accurate approach for the procedural blank correction. It is similar in principle to the description given in Sect. 4.1.2 for air standards and based on Eq. (2). We used 0.5 ± 0.2 mVs, -27 ± 1 ‰ and -29 ± 3 ‰ for procedural blank size, $\delta^{13}C$ and $\delta^{18}O$, respectively (Sect. 4.1.2). Results and the achieved precision for measurements of natural ice sample can be found in Sect. 4.2.2.

4.2 System performance

4.2.1 Precision of analytical system for the measurement of air samples

The precision and long term consistency of our measurements was assessed by repeated quality control sample (QCS) measurements of the two air standards AL–1 and AL–2 injected over natural and artificial (BFI) both before and after crushing. These two standards are different in their CO_2 mixing ratio and isotopic composition and were injected in variable amounts of gas. QCS were treated similar to a real ice samples both in the applied measurement procedure (except for the crushing step) and the post-processing of the acquired raw data. In Fig. 6, the resulting time series for CO_2, $\delta^{13}C$ and $\delta^{18}O$ covering a two year period are shown. To derive a completely independent assessment, QCS measurement used in the daily calibration routine were excluded for this analysis. For the time frame covered, no trend can be observed for either of the parameters analyzed in the two standards and determined and assigned values agree well within the uncertainties. However, a small systematic shift of unknown origin observed for $\delta^{18}O$ of AL–2 cannot be excluded. From the combined dataset of AL–1 and AL–2 shown in Fig. 6, the precision of the analytical system for the measurement of air samples over ice was determined with 1.9 ppm, 0.09 ‰ and 0.16 ‰ for CO_2, $\delta^{13}C$ and $\delta^{18}O$, respectively (standard deviations around the respective mean).

4.2.2 Natural ice samples – laboratory comparison and reproducibility

From measurements of ice samples of 8–13 g from various sites and depths, the extraction efficiency (i.e. the amount of air liberated divided by total air in the sample) of our NC was determined to be typically around 70–80 % for bubbly ice and around 60 % for clathrate ice

Atmos. Meas. Tech. Discuss., doi:10.5194/amt-2015-351, 2016
Manuscript under review for journal Atmos. Meas. Tech.
Published: 1 February 2016

Atmospheric Measurement Techniques Discussions

(with the gas release time after crushing extended by four minutes). This is in the similar range as reported for other NC designs (Ahn et al., 2009; Lüthi, 2009).

To demonstrate system performance and reproducibility we analyzed six ice samples of the recent past (1851–1969 AD) from Law Dome, Antarctica (DE08, 66°43'S, 113°12'E). This was done in a comparison study with CSIRO. The range of sample ages allows for a comparison across a range of CO_2 and $\delta^{13}C$ values. These samples were also part of an independent study published earlier (Rubino et al., 2013). Note that DE08 was drilled without the use of fluid and therefore the difference in the measurement systems that addresses drilling fluid contamination (i.e. separation by GC in the CIC system) is not tested. We measured replicates (n = 2 or 3) on the egg-shaped leftover pieces remaining after the samples have been processed at CSIRO using their Cheese Grater dry extraction system. To allow assessment of measurement reproducibility, the replicates were measured on different days resulting in a pooled standard deviation of 2.0 ppm and 0.11 ‰ for CO_2 and $\delta^{13}C$, respectively. Compared with the results from CSIRO, good agreement within the assigned 1σ uncertainties was found for both CO_2 and $\delta^{13}C$ (Fig. 7). Whereas the agreement (CIC - CSIRO average) between $\delta^{13}C$ results is high with +0.02 ‰, a small systematic offset of +1.8 ppm seems to exist for CO_2. An obvious explanation for this offset would be discrepancies in calibration between the two laboratories relying on independent standards. This is however not supported by the good agreement for the comparison of air tank measurements with different CO_2 mixing ratios (-0.3 ppm on average, n = 3) although not to be completely ruled out because a precise quantification is not possible with the assigned uncertainties. Alternatively, the observed offset could be a real signal, explained by the occlusion of recent air in micro-cracks resulting from the fierce mechanical treatment in the CSIRO grater and the elevated temperatures (around -5°C) during ice transport preceding the measurements at CIC. For the same reason, the deviation in results of replicate measurements may be influenced by the ice itself, i.e. causing analytically independent variability. We therefore consider the pooled standard deviation calculated from the Law Dome samples to be a rather conservative estimate of the overall analytical uncertainty for single measurements. The estimate is in line with the uncertainty determined for the QCS measurements (Sect. 4.2.1). The slightly larger uncertainty determined here can be expected for the measurements of ice due to the procedural blank correction being bigger both in size and uncertainty compared to the system blank correction applied to the QCS. Due to the benefit of the small sample size required by our method, execution of replicate measurements is feasible even though the

Atmos. Meas. Tech. Discuss., doi:10.5194/amt-2015-351, 2016
Manuscript under review for journal Atmos. Meas. Tech.
Published: 1 February 2016

availability of samples from ice cores is limited. Therefore, the achievable overall method precision for a measurement based on *n* ice sample replicates is increased by $(n)^{-0.5}$ compared to the defined uncertainty for a single measurement. For $\delta^{18}O$ the pooled standard deviation is 0.32 ‰ and the offset between the two laboratories was 0.5 ‰ on average (Fig. S4). However, oxygen exchanges between CO_2 and H_2O from the surrounding ice matrix (Friedli et al., 1984; Siegenthaler et al., 1988; Assonov et al., 2005; Bauska et al., 2014). Because variation in $\delta^{18}O$-H_2O due to the seasonal cycle has to be expected even for the high CIC sampling resolution (see Sect. 4.3) analytically independent variability will result for $\delta^{18}O$-CO_2 results of replicates. This effect might at least partly explain the 2 times higher variation compared to the QCS results (Sect. 4.2.1) as well as the difference between the laboratory $\delta^{18}O$-CO_2 results regarding the large difference in sample size and resolution used for CSIRO and CIC measurements.

4.3 Outlier detection based on $\delta^{18}O$-CO_2 and $\delta^{18}O$-H_2O

CO_2 exchange with the terrestrial biosphere dominates the signal of the $^{18}O/^{16}O$ ratio in atmospheric CO_2. Therefore, atmospheric ^{18}O-CO_2 is a valuable proxy to constrain changes in terrestrial primary production and the hydrological cycle (e.g. Farquhar et al., 1993). However, ^{18}O-CO_2 measured in ice core samples is affected by the exchange of oxygen with the ice matrix. This has been demonstrated by measurements on big ice samples (> 100 g) for different sites and time periods (Friedli et al., 1984; Siegenthaler et al., 1988; Assonov et al., 2005; Bauska et al., 2014) as well as in firn gas (Assonov et al., 2005).

Here, we present a new approach for analytical quality control, based on $\delta^{18}O$-CO_2 measurements. It allows reliable and consistent rejection of results from samples which were affected by analytical problems or suffered contamination during e.g. storage or measurement extraction. Different sections (bags) from GRIP and NGRIP with gas ages of 260 to 1770 years (bags GRIP–250, –360 and NGRIP–213, –696) and 25'000 years (bags GRIP–3628, –3636) were analyzed in high spatial and temporal resolution of 2.5 cm and < 1 year (ice age scale), respectively. Parallel samples (same depth) were measured for $\delta^{18}O$-H_2O in similar resolution where no data already existed. From the $\delta^{18}O$-H_2O data the expected $\delta^{18}O$-CO_2 was calculated considering the thermodynamic equilibrium of gaseous CO_2 with the surrounding ice matrix, in the following denoted as $\delta^{18}O$-$(CO_2\text{-ice})_{eq}$. We thereby followed Siegenthaler et al. (1988) using the fractionation factors for H_2O phase change given therein. The time to reach 50 % of the thermodynamic equilibrium ($T^1/_2$) was empirically determined

Atmos. Meas. Tech. Discuss., doi:10.5194/amt-2015-351, 2016
Manuscript under review for journal Atmos. Meas. Tech.
Published: 1 February 2016

Atmospheric Measurement Techniques Discussions

to be 23 years for a site with annual mean temperatures of -26°C (Berkner, Antarctica), comparable to the site temperatures at GRIP and NGRIP (Assonov et al., 2005). It is therefore safe to assume that even the youngest samples analyzed here in this study have reached complete equilibrium in the glacier. However, the GRIP and NGRIP ice cores were drilled in 1992 and from 1996–2004, respectively. From the time the cores have been recovered, a new thermodynamic equilibrium now driven by the storage temperature needs to be considered. For $T^1/_2$ and storage duration of ~15 and 20 years until the time of measurement, this new equilibrium has only been reached to 30 % and 45 % for NGRIP and GRIP samples, respectively. To take this into account, the equilibrium temperature was defined as the weighted mean of borehole temperature at sampling site depth (around -30°C; Johnsen et al., 1995; Dahl-Jensen et al., 2003) and freezer temperature (-23 °C) with the weighting of freezer temperature being 0.30 and 0.45 for NGRIP and GRIP, accordingly. The uncertainty of the equilibrium temperature was estimated assuming an uncertainty of 10 % for the state of the equilibrium and 2 °C each for borehole and storage temperatures. In Fig. 8, the correlation between measured and expected $\delta^{18}O\text{-}CO_2$ is shown (Fig. S5 shows measured $\delta^{18}O\text{-}CO_2$ and $\delta^{18}O\text{-}H_2O$ on their respective scales for one of the sections analyzed). Overall, the measured and theoretical values agree well and are highly correlated (R = 0.90) which confirms the exchange of oxygen between CO_2 and H_2O within the ice archive as observed in the studies cited above. The 1σ standard deviation around the measured equilibrium line was 0.8 ‰, exceeding the estimated analytical precision by more than a factor of two. Based on that, we defined an outlier identification criteria for samples where $\delta^{18}O\text{-}CO_2$ measurements differed by more than 1.6 ‰ (2σ) from the theoretical value. Results for CO_2 and $\delta^{13}C$ of such samples were then rejected.

5 Conclusions and outlook

This study describes a new analytical setup for simultaneous measurements of atmospheric CO_2 mixing ratios, atmospheric $\delta^{13}C$ and $\delta^{18}O\text{-}CO_2$ in air extracted from ice core samples. The core of the system is a newly designed Needle Cracker for mechanical dry extraction, operated at an extra low temperature of -45 °C. With this setup the throughput is four samples per day and the small amount of ice required (8–13 g) allows high resolution sampling schemes.

Atmos. Meas. Tech. Discuss., doi:10.5194/amt-2015-351, 2016
Manuscript under review for journal Atmos. Meas. Tech.
Published: 1 February 2016

Atmospheric Measurement Techniques Discussions

We discussed analytical procedures, systematic linearity testing for the various system parts, daily calibration as well as data processing. Determined from repeated long-term quality control measurement of air samples over ice (natural or BFI), the analytical precision of the presented system resulted with 1.9 ppm for CO_2 and 0.09 ‰ for $\delta^{13}C$. Law Dome ice core samples were analyzed in a laboratory intercomparison study with CSIRO and good agreement between the two laboratories was found for CO_2 and $\delta^{13}C$. Replicate analysis of these samples was performed on different days and resulted in a pooled standard deviation of 2.0 ppm for CO_2 and 0.11 ‰ for $\delta^{13}C$. These numbers are rather conservative estimates of the overall analytical uncertainty for single measurement. The achievable method precision is higher for the results of replicate measurements which are feasible because of the small sample requirement of the system. In conclusion, our system is well calibrated and precision comparable to others systems using samples of similar small sizes.

Further, a new approach was proposed for the correction of the procedural blank leading to more accurate results particularly for the measurements of small samples. Analysis of $\delta^{18}O$-CO_2 and $\delta^{18}O$-H_2O confirmed the previously observed exchange of oxygen between CO_2 and the surrounding ice matrix occurring within the archive. Based on this, we introduced a new approach for analytical outlier detection which allows reliable and consistent rejection of results from samples affected by analytical problems or some sort of contamination.

Methodological improvement could be achieved from higher extraction efficiency (clathrate ice) and further reduction in system blank size. Increased system automation (gas manifold, vacuum lines) and optimization of dimensions for connection lines and traps could be favourable.

Acknowledgements

This work was partly funded by the Centre for Ice and Climate through the Danish National Research Foundation (DNRF) and the European Union's Seventh Framework programme (FP7/2007-2013) under grant agreement no 243908, "Past4Future. Climate change - Learning from the past climate." CSIRO's contribution was supported in part by the Australian Climate Change Science Program, an Australian Government Initiative. Thanks belong to the teams involved in recovering and analysis of GRIP, NGRIP and Law Dome sample. We highly appreciate the excellent work done at the Niels Bohr Institute workshop of the Copenhagen University. Special thank belongs to Erik Kaimer for help with all the technical aspects of the

Atmos. Meas. Tech. Discuss., doi:10.5194/amt-2015-351, 2016
Manuscript under review for journal Atmos. Meas. Tech.
Published: 1 February 2016

Atmospheric Measurement Techniques Discussions

NC design and to Carsten Mortensen, Alex Boisen, Jørgen Jørgensen, Morten Christensen, Dennis Westphal Wistisen and Simon Sheldon for final manufacturing of the unit, the production of various system components and technical support. Credit goes to Trevor Popp and Bo M. Vinther from the CIC stable isotope laboratory for $\delta^{18}O$-H_2O data and measurements and to Colin Allison, Scott Coram and Ray Langenfelds for their contribution related to CSIRO gas measurements. Thanks also belong to Peter Sperlich, Christo Buizert, Christopher Stowasser, Myriam Guillevic and Correntin Reutenauer for discussions, input and all the hours spent in the laboratory. Finally, many thanks to the entire CIC team for scientific exchange and the excellent working environment, particularly to Dorthe Dahl-Jensen who made this all happen.

Atmos. Meas. Tech. Discuss., doi:10.5194/amt-2015-351, 2016
Manuscript under review for journal Atmos. Meas. Tech.
Published: 1 February 2016

Atmospheric Measurement Techniques Discussions

References

Ahn, J. H., Brook, E. J., and Howell, K.: A high-precision method for measurement of paleoatmospheric CO_2 in small polar ice samples, Journal of Glaciology, 55, 191, 499-506, 2009.

Anklin, M., Barnola, J.-M., Schwander, J., Stauffer, B., and Raynaud, B.: Processes affecting the CO_2 concentrations measured in Greenland ice, Tellus, 47 B, 461-470, 1995.

Assonov, S. S., Brenninkmeijer, C. A. M., and Jöckel, P.: The ^{18}O isotope exchange rate between firn air CO_2 and the firn matrix at three Antarctic sites, Journal of Geophysical Research: Atmospheres, 110, D18310, 10.1029/2005JD005769, 2005.

Barnola, J.-M., Anklin, M., Porcheron, J., Raynaud, D., Schwander, J., and Stauffer, B.: CO_2 evolution during the last millenium as recorded by Antarctic and Greenland ice, Tellus, 47B, 264-272, 1995.

Bauska, T. K., Brook, E. J., Mix, A. C., and Ross, A.: High-precision dual-inlet IRMS measurements of the stable isotopes of CO_2 and the N_2O/CO_2 ratio from polar ice core samples, Atmos. Meas. Tech., 7, 11, 3825-3837, 10.5194/amt-7-3825-2014, 2014.

Bereiter, B., Eggleston, S., Schmitt, J., Nehrbass-Ahles, C., Stocker, T. F., Fischer, H., Kipfstuhl, S., and Chappellaz, J.: Revision of the EPICA Dome C CO_2 record from 800 to 600 kyr before present, Geophysical Research Letters, 42, 2, 542-549, 10.1002/2014gl061957, 2015.

Bereiter, B., Fischer, H., Schwander, J., and Stocker, T. F.: Diffusive equilibration of N_2, O_2 and CO_2 mixing ratios in a 1.5 million years old ice core, The Cryosphere Discuss, 7, 2029-2060, 2013a.

Bereiter, B., Stocker, T. F., and Fischer, H.: A centrifugal ice microtome for measurements of atmospheric CO_2 on air trapped in polar ice cores, Atmos. Meas. Tech., 6, 2, 251-262, 10.5194/amt-6-251-2013, 2013b.

Berner, W., Oeschger, H., and Stauffer, B.: Information on the CO_2 cycle from ice core studies, Radiocarbon, 22, 2, 227-235, 1980.

Dahl-Jensen, D., Gundestrup, N., Gorgineni, S. P., and Miller, H.: Basal melt at NorthGRIP modeled from borehole, ice-core and radio-echo sounder observations, Annals of Glaciology, 37, 207-212, 2003.

Delmas, R. J., Ascencio, J.-M., and Legrand, M.: Polar ice evidence that atmospheric CO_2 20,000 yr BP was 50% of present, Nature, 284, 155-157, 1980.

Elsig, J. and Leuenberger, M. C.: ^{13}C and ^{18}O fractionation effects on open splits and on the ion source in continuous flow isotope ratio mass spectrometry, Rapid Communications in Mass Spectrometry, 24, 10, 1419-1430, 10.1002/rcm.4531, 2010.

Elsig, J., Schmitt, J., Leuenberger, D., Schneider, R., Eyer, M., Leuenberger, M., Joos, F., Fischer, H., and Stocker, T. F.: Stable isotope constraints on Holocene carbon cycle changes from an Antarctic ice core, Nature, 461, 7263, 507-510, 2009.

Etheridge, D. M., Steele, L. P., Langenfields, R. L., Francey, R. J., Barnola, J.-M., and Morgan, V. I.: Natural and anthropogenic changes in atmospheric CO_2 over the last 1000 years from air in Antarctic ice and firn, Journal of Geophysical Research, 101, 4115-4128, 1996.

Farquhar, G. D., Lloyd, J., Taylor, J. A., Flanagan, L. B., Syvertsen, J. P., Hubick, K. T., Wong, S. C., and Ehleringer, J. R.: Vegetation Effects on the Isotope Composition of Oxygen in Atmospheric CO_2, Nature, 363, 6428, 439-443, 10.1038/363439a0, 1993.

Francey, R. J., Allison, C. E., Etheridge, D. M., Trudinger, C. M., Enting, I. G., Leuenberger, M., Langenfelds, R. L., Michel, E., and Steele, L. P.: A 1000-year high precision record of $\delta^{13}C$ in atmospheric CO_2, Tellus Ser. B-Chem. Phys. Meteorol., 51B, 2, 170-193, 10.1034/j.1600-0889.1999.t01-1-00005.x, 1999.

Friedli, H., Moor, E., Oeschger, H., Siegenthaler, U., and Stauffer, B.: $^{13}C/^{12}C$ ratios in CO_2 extracted from Antarctic ice, Geophysical Research Letters, 11, 11, 1145-1148, 10.1029/GL011i011p01145, 1984.

Güllük, T., Slemr, F., and Stauffer, B.: Simultaneous measurements of CO_2, CH_4 and N_2O in air extracted by sublimation from Antarctica ice cores: confirmation of the data obtained using other extraction techniques, Journal of Geophysical Research, 103, D13, 15971-15978, 1998.

Ikeda, T., Fukazawa, H., Mae, S., Pépin, L., Duval, P., Champagnon, B., Lipenkov, V. Y., and Hondoh, T.: Extreme fractionation of gases caused by formation of clathrate hydrates in Vostok Antarctic ice, Geophysical Research Letters, 26, 1, 91-94, 1999.

Indermühle, A., Stocker, T. F., Fischer, H., Smith, H. J., Joos, F., Wahlen, M., Deck, B., Mastroianni, D., Tschumi, J., Blunier, T., Meyer, R., and Stauffer, B.: Holocene carbon-cycle dynamics based on CO_2 trapped in ice at Taylor Dome, Antarctica, Nature, 398, 121-126, 1999.

Johnsen, S., Dahl-Jensen, D., Dansgaard, W., and Gundestrup, N.: Greenland palaeotemperatures derived from GRIP bore hole temperature and ice core isotope profiles, Tellus B, 47, 5, 624-629, 1995.

Kawamura, K., Nakazawa, T., Aoki, S., Sugawara, S., Fujii, Y., and Watanabe, O.: Atmospheric CO_2 variations over the last three glacial–interglacial climatic cycles deduced from the Dome Fuji deep ice core, Antarctica using a wet extraction technique, Tellus B, 55, 2, 126-137, 2003.

Köhler, P., Fischer, H., Schmitt, J., and Munhoven, G.: On the application and interpretation of Keeling plots in paleo climate research – deciphering $\delta^{13}C$ of atmospheric CO_2 measured in ice cores, Biogeosciences, 3, 4, 539-556, 10.5194/bg-3-539-2006, 2006.

Leuenberger, D.: Highly resolved measurements of $\delta^{13}C$ on CO_2 extracted from an EPICA Dome C ice core, Master Thesis, Division for Climate and Environmental Physics, Physics Institute and Oeschger Centre for Climate Change Research, University of Bern, 2009.

Lourantou, A.: Constraints on the carbon dioxide deglacial rise based on its stable carbon isotopic ratio, Ph.D. thesis, doi: Univ. Joseph Fourier, Grenoble, France, 2009. Univ. Joseph Fourier, Grenoble, France, Univ. Joseph Fourier, Grenoble, France, 2009.

Lourantou, A., Chappellaz, J., Barnola, J. M., Masson-Delmotte, V., and Raynaud, D.: Changes in atmospheric CO_2 and its carbon isotopic ratio during the penultimate deglaciation, Quaternary Science Reviews, 29, 17-18, 1983-1992, 10.1016/j.quascirev.2010.05.002, 2010a.

Lourantou, A., Lavric, J. V., Kohler, P., Barnola, J. M., Paillard, D., Michel, E., Raynaud, D., and Chappellaz, J.: Constraint of the CO_2 rise by new atmospheric carbon isotopic

measurements during the last deglaciation, Global Biogeochemical Cycles, 24, Gb2015, 10.1029/2009gb003545, 2010b.

Lüthi, D.: CO_2 Konzentrationsmessungen an antarktischen Eisohrkernen: Natürliche Variabilität der letzten 800'000 Jahre und deren Zuverlässigkeit in Anbetracht von Prozessen im Eis, Dissertation, Physikalisches Institut, Abteilung Klima- und Umweltphysik, University of Bern, 160 pp., 2009.

Lüthi, D., Le Floch, M., Bereiter, B., Blunier, T., Barnola, J.-M., Siegenthaler, U., Raynaud, D., Jouzel, J., Fischer, H., and Kawamura, K.: High-resolution carbon dioxide concentration record 650,000–800,000 years before present, Nature, 453, 7193, 379-382, 2008.

MacFarling Meure, C.; Etheridge, D.; Trudinger, C.; Steele, P.; Langenfelds, R.; van Ommen, T.; Smith, A. and Elkins, J.: Law Dome CO_2, CH_4 and N_2O ice core records extended to 2000 years BP, Geophysical Research Letters, 33, L14810, doi:10.1029/2006GL026152, 2006.

Meijer, H. A. J.: The isotopic composition of the Groningen GS-19 and GS-20 pure CO_2 standards, in Reference and intercomparison materials for stable isotopes of lightelements, IAEA-TECDOC-825, 81-83, International Atomic Energy Agency, Vienna, 1995.

Neftel, A., Oeschger, H., Schwander, J., Stauffer, B., and Zumbrunn, R.: Ice core sample measurements give atmospheric CO_2 content during the past 40,000 yr, Nature, 295, 220-223, 1982.

Pearman, G. I., Etheridge, D., de Silva, F., and Fraser, P. J.: Evidence of changing concentrations of atmospheric CO_2, N_2O and CH_4 from air bubbles in Antarctic ice, Nature, 320, 6059, 248-250, 1986.

Rubino, M., Etheridge, D. M., Trudinger, C. M., Allison, C. E., Battle, M. O., Langenfelds, R. L., Steele, L. P., Curran, M., Bender, M., White, J. W. C., Jenk, T. M., Blunier, T., and Francey, R. J.: A revised 1000 year atmospheric $\delta^{13}C$-CO_2 record from Law Dome and South Pole, Antarctica, Journal of Geophysical Research: Atmospheres, 118, 15, 8482-8499, 10.1002/jgrd.50668, 2013.

Schaefer, H., Lourantou, A., Chappellaz, J., Lüthi, D., Bereiter, B., and Barnola, J.-M.: On the suitability of partially clathrated ice for analysis of concentration and $\delta^{13}C$ of palaeo-

atmospheric CO_2, Earth and Planetary Science Letters, 307, 3-4, 334-340, 10.1016/j.epsl.2011.05.007, 2011.

Schmitt, J.: A sublimation technique for high-precision $\delta^{13}C$ on CO_2 and CO_2 mixing ratio from air trapped in deep ice cores, Dissertation, University of Bremen, 2006.

Schmitt, J., Schneider, R., and Fischer, H.: A sublimation technique for high-precision $\delta^{13}C$ on CO_2 and CO_2 mixing ratio from air trapped in deep ice cores, Atmos. Meas. Tech., 4, 1445-1461, 2011.

Schneider, R., Schmitt, J., Koehler, P., Joos, F., and Fischer, H.: A reconstruction of atmospheric carbon dioxide and its stable carbon isotopic composition from the penultimate glacial maximum to the last glacial inception, Climate of the Past, 9, 6, 2507-2523, 10.5194/cp-9-2507-2013, 2013.

Siegenthaler, U., Friedli, H., Loetscher, H., Moor, E., Neftel, A., Oeschger, H., and Stauffer, B.: Stable-isotope ratios and concentration of CO_2 in air from polar ice cores, Annals of Glaciology, 10, 151-156, 1988.

Smith, H. J., Fischer, H., Wahlen, M., Mastroianni, D., and Deck, B.: Dual modes of the carbon cycle since the Last Glacial Maximum, Nature, 400, 6741, 248-250, 10.1038/22291, 1999.

Sowers, T. and Jubenville, J.: A modified extraction technique for liberating occluded gases from ice cores, Journal of Geophysical Research-Atmospheres, 105, D23, 29155-29164, 2000.

Sperlich, P., Buizert, C., Jenk, T. M., Sapart, C. J., Prokopiou, M., Röckmann, T., and Blunier, T.: An automated GC-C-GC-IRMS setup to measure palaeoatmospheric $\delta^{13}C$-CH_4, $\delta^{15}N$-N_2O and $\delta^{18}O$-N_2O in one ice core sample, Atmos. Meas. Tech., 6, 8, 2027-2041, 10.5194/amt-6-2027-2013, 2013.

Stauffer, B., Fischer, G., Neftel, A., and Oeschger, H.: Increase of Atmospheric Methane Recorded in Antarctic Ice Core, Science, 229, 1386-1388, 1985.

Stowasser, C., Buizert, C., Gkinis, V., Chappellaz, J., Schüpbach, S., Bigler, M., Faïn, X., Sperlich, P., Baumgartner, M., Schilt, A., and Blunier, T.: Continuous measurements of

methane mixing ratios from ice cores, Atmos. Meas. Tech., 5, 5, 999-1013, 10.5194/amt-5-999-2012, 2012.

Sturm, P., Leuenberger, M., Sirignano, C., Neubert, R., Meijer, H., Langenfelds, R., Brand, W., and Tohjima, Y.: Permeation of atmospheric gases through polymer O-rings used in flasks for air sampling, Journal of Geophysical Research: Atmospheres (1984–2012), 109, D4, 2004.

Tans, P. P. and Zhao, C. L.: Maintenance and propagation of the WMO mole fraction scale for carbon dioxide in air, 12th WMO/IAEA Meeting of Experts on Carbon Dioxide Concentration and Related Tracer Measurements Techniques, World Meteorological Organisation, Toronto, Ontario, Canada, 2003.

Trudinger, C. M., Enting, I. G., Francey, R. J., Etheridge, D. M., and Rayner, P. J.: Long-term variability in the global carbon cycle inferred from a high-precision CO_2 and $\delta^{13}C$ ice-core record, Tellus Series B-Chemical and Physical Meteorology, 51, 2, 233-248, 10.1034/j.1600-0889.1999.t01-1-00009.x, 1999.

Uchida, T., Hondoh, T., Mae, S., Shoji, H., and Azuma, N.: Optimized storage condition of deep ice core samples from the viewpoint of air-hydrate analysis, Mem. Natl Inst. Polar Res., Spec. Issue 49, 306-313, 1994.

Werner, R. A. and Brand, W. A.: Referencing strategies and techniques in stable isotope ratio analysis, Rapid Communications in Mass Spectrometry, 15, 7, 501-519, 2001.

Zhang, J., Quay, P. D., and Wilbur, D. O.: Carbon isotope fractionation during gas-water exchange and dissolution of CO_2, Geochim. Cosmochim. Acta, 59, 1, 107-114, 1995.

Zhao, C. L. and Tans, P. P.: Estimating uncertainty of the WMO mole fraction scale for carbon dioxide in air, Journal of Geophysical Research: Atmospheres, 111, D08S09, 10.1029/2005JD006003, 2006.

Zumbrunn, R., Neftel, A., and Oeschger, H.: CO_2 measurements on 1-cm^3 ice samples with an IR laserspectrometer (IRLS) combined with a new dry extraction device, Earth and Planetary Science Letters, 60, 318-324, 1982.

Atmos. Meas. Tech. Discuss., doi:10.5194/amt-2015-351, 2016
Manuscript under review for journal Atmos. Meas. Tech.
Published: 1 February 2016

Atmospheric Measurement Techniques Discussions

Table 1: CIC standards used for referencing CO_2 mixing and stable isotope ratios.

Name	Reference	Gas	CO_2 (ppm)	$\delta^{13}C$-CO_2 (‰ VPDB)	$\delta^{18}O$-CO_2 (‰ VPDB-CO_2)
Messer–649250 [1]	GS19/GS20	CO_2		-6.004 ± 0.008	-10.80 ± 0.13
CA08274 [2,3]	NOAA/CIC	Air	181.04 ± 0.06	(-35) [#]	(-32) [#]
CA08054 [2,4]	NOAA	Air	267.08 ± 0.01	-7.779 ± 0.002	-7.531 ± 0.005
CA08292 [2,3]	NOAA/CIC	Air	400.53 ± 0.02	(-35) [#]	(-31) [#]
AL–1 [3,5]	CIC	Air	215.8 ± 0.7	-9.26 ± 0.04	-8.02 ± 0.07
AL–2 [3,5]	CIC	Air	368.9 ± 0.5	-9.80 ± 0.02	-9.73 ± 0.08
NEEM–2 [3,5]	CIC	Air	378.6 ± 0.5	-8.0 ± 0.1	0.1 ± 0.1

[1] Stable isotopic composition calibrated at CIC by IRMS Dual Inlet against GS19 and GS20 (Centre for Isotope Research, Gröningen University, Netherlands). [2] CO_2 mixing ratio calibrated and certified by the NOAA ESRL Global Monitoring Division (Boulder, Colorado USA). [3] Stable isotopic composition calibrated at CIC against Messer–649250 and CA08054 with the setup described in this study but in "dry mode" (without ice). [4] Stable isotopic composition calibrated by the Stable Isotope Lab (SIOL) at INSTAAR (University of Colorado, USA) in cooperation with the NOAA ESRL Global Monitoring Division. [5] CO_2 mixing ratio calibrated at CIC against the three NOAA standards CA08274, CA08054 and CA08292 with the setup described in this study and by laser spectrometry measurements (Picarro Inc., USA). [#] Values outside of the reliable calibration range.

Atmos. Meas. Tech. Discuss., doi:10.5194/amt-2015-351, 2016
Manuscript under review for journal Atmos. Meas. Tech.
Published: 1 February 2016

Table 2: Example of a daily measurement sequence. BFI stands for bubble free ice. See Table 1 for details on standard gases and text for analytical procedures.

Daily run	Type of sample	Sample name	Comment	Setup[#]	Data processing[§]
1	WS - 0.4 µl	Messer–649250	1st run of the day	B	*(discard)*
2	Blank	Blank		B	determination/control of blank
3	WS - 0.4 µl	Messer–649250	1st run after blank	B	*(discard)*
4	WS - 0.2 µl	Messer–649250		B	control of day to day stability (drift and size dependency)
5	WS - 0.4 µl	Messer–649250		B	
6	Air Std	CA08054	sample loaded - NC opened	A, B	*(discard, NC surface effects)*
7	Air Std	CA08054		A, B	*(discard)*
8	Air Std	CA08054		A, B	daily calibration & drift correction
9	ICE	DE08–439	ice crushed	A, B	RESULT
10	Air Std	CA08054		A, B	daily calibration & drift correction
11	Air Std	CA08054	sample loaded - NC opened	A, B	*(discard, NC surface effects)*
12	ICE (or BFI)*	GRIP 250–12 (BFI (+ CA08054)*)*	ice crushed (not crushed)*	A, B	RESULT (determ./control of procedural blank)*
13	Air Std	CA08054		A, B	daily calibration & drift correction
14	Air Std	CA08054	sample loaded - NC opened	A, B	*(discard, NC surface effects)*
15	ICE	DE08–443	ice crushed	A, B	RESULT
16	Air Std	AL–2		A, B	daily calibration
17	Air Std	AL–1 (AL–2)*		A, B	quality control sample (QCS)
18	Air Std	CA08054	sample loaded - NC opened	A, B	*(discard, NC surface effects)*
19	ICE	DE08–426	ice crushed	A, B	RESULT
20	Air Std	CA08054		A, B	daily calibration & drift correction
21	Air Std	AL–1 (CA08292/CA08274)*		A, B	daily calibration
(21)*	Air Std	CA08054	different injection size	A, B	control of size independency

[#]Section of system passed by the analyzed gas sample (see Fig. 2). *Alternative possibility of gas typically measured at this position of the sequence. [§]See text for details about data processing.

Atmos. Meas. Tech. Discuss., doi:10.5194/amt-2015-351, 2016
Manuscript under review for journal Atmos. Meas. Tech.
Published: 1 February 2016

Atmospheric Measurement Techniques Discussions

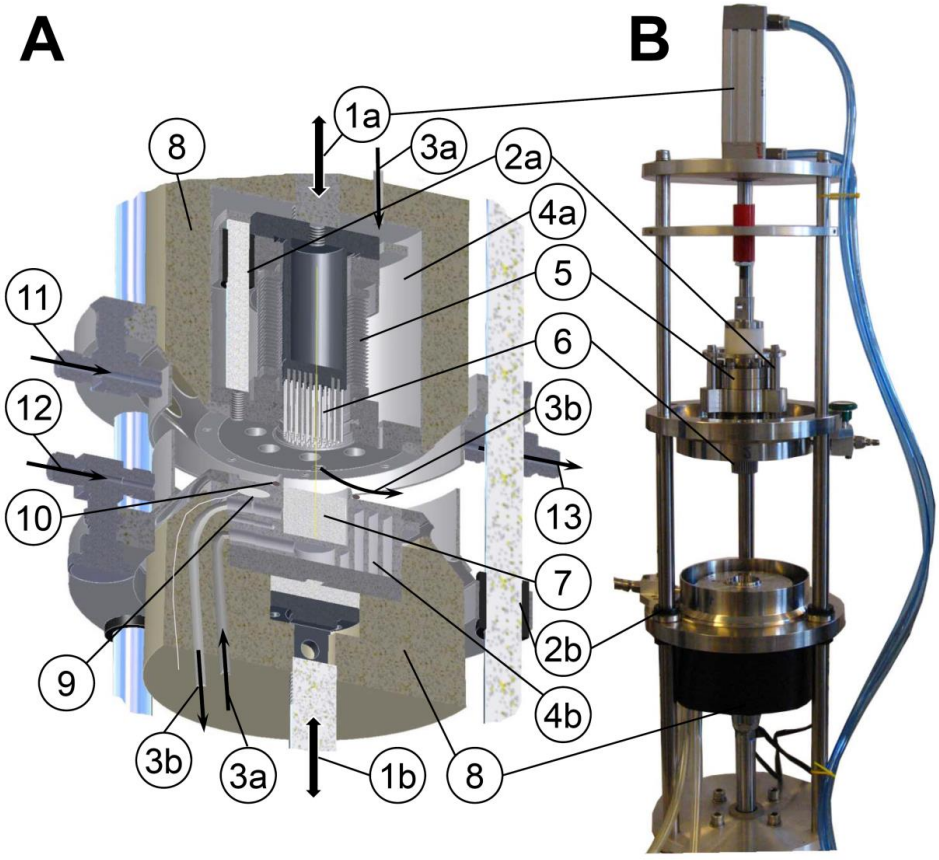

Figure 1: A) Schematic of the CIC Needle Cracker (NC) dry extraction unit and B) picture with cooling jacket and insulation dismounted at the top part. Pneumatic actuators (1a, 1b), guiding SST rods with bearings (2a, 2b), cold air inlet and outlet for cooling (3a and 3b respectively), cooling jacket and cooling cavities (4a and 4b, respectively), SST welded bellow (5), SST needle pins (6), ice sample (7), insulation (8), temperature sensor (9), indium wire for vacuum seal (10), gas inlets and outlet (11, 12 and 13, respectively).

Atmos. Meas. Tech. Discuss., doi:10.5194/amt-2015-351, 2016
Manuscript under review for journal Atmos. Meas. Tech.
Published: 1 February 2016

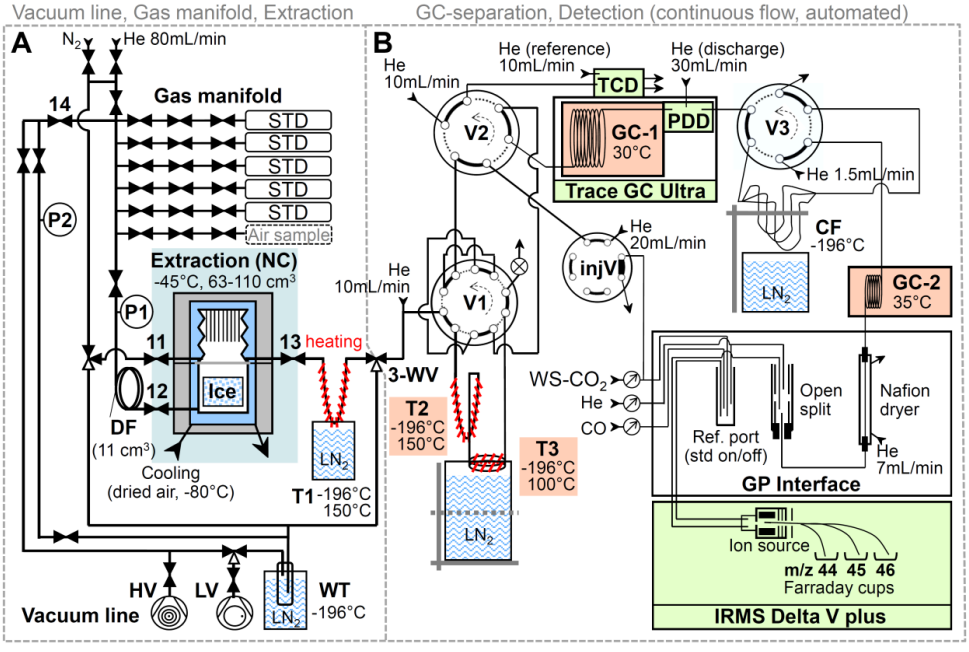

Figure 2: Schematic representation of the new analytical CIC system for simultaneous measurements of CO_2 mixing and stable isotope ratios. The setup consists of a manually operated section (A) allowing injection and loading of air and ice samples, respectively and a fully automated section (B) for gas separation, purification and final detection which is run in a continuous flow mode. Highlighted in red and green are the components for gas separation and detection, respectively. See text for more details.

Atmos. Meas. Tech. Discuss., doi:10.5194/amt-2015-351, 2016
Manuscript under review for journal Atmos. Meas. Tech.
Published: 1 February 2016

Atmospheric Measurement Techniques Discussions

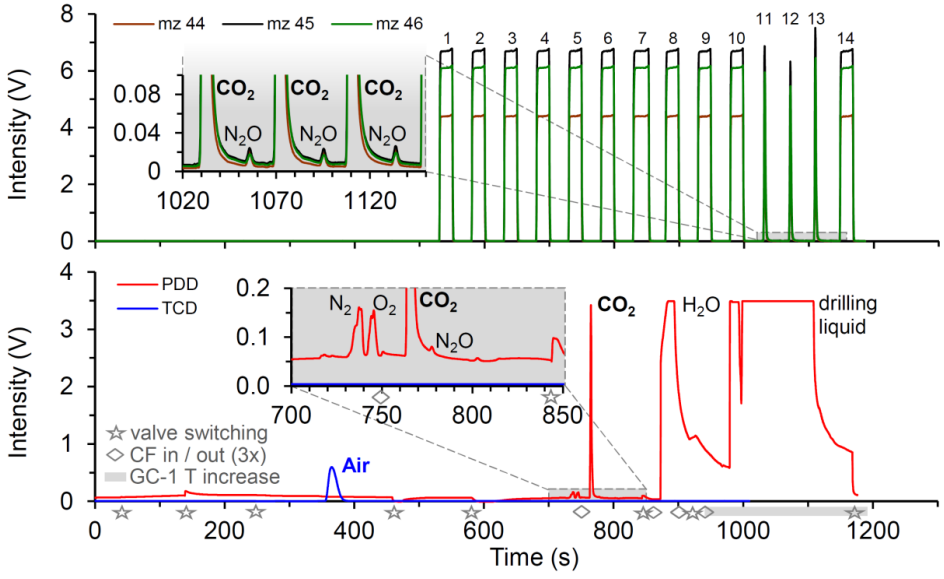

Figure 3: Chromatograms for the measurement of an ice sample as described in Sect. 3.2. Upper panel: IRMS signal intensity for mass 44, 45, and 46. The flat-topped peaks are on/off peaks of the CO_2-WS injected via the open split. Peaks 1–9 are used to reach stable source conditions while peaks 10 and 14 before and after the samples are used for referencing. The inset shows baseline details and N_2O separation in detail. Lower panel: PDD and TCD intensity signal for CO_2 and air, respectively. Stars indicate valve switching, resulting in small variations in the PDD signal due to changes in pressure and flow (see inset, not detected by the less sensitive TCD). Diamonds indicate immersion of the three capillary traps into liquid nitrogen for CO_2 cryofocusing and their subsequent one by one release resulting in the three peaks of the split sample shown in the upper panel (peaks 11–13). Over the time period indicated by the grey bar the GC–1 temperature is increased to 150 °C in order to pre-condition the column for the next sample (release of water and remnants of drilling liquid contamination). The enlargement shows baseline details revealing the N_2O peak and small remains of N_2 and O_2 from the air sample, incompletely separated by the preceding cryogenic partition.

Atmos. Meas. Tech. Discuss., doi:10.5194/amt-2015-351, 2016
Manuscript under review for journal Atmos. Meas. Tech.
Published: 1 February 2016

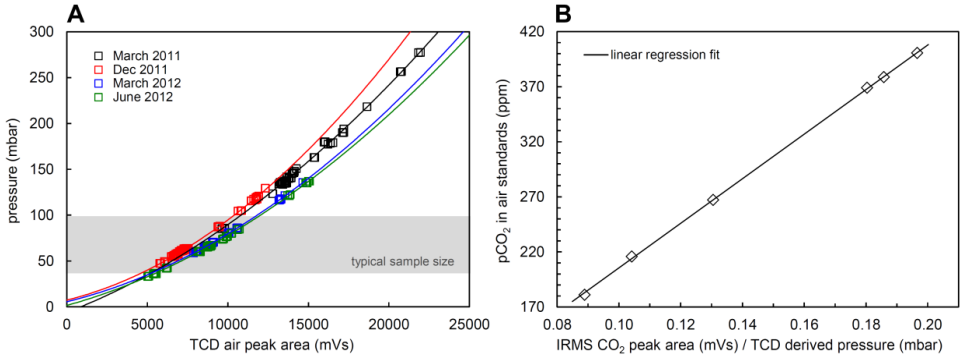

Figure 4: CO_2 calibration. A) Relationship between sample size and TCD peak area of air for different measurement periods. The lines are second order polynomial fits through the data. Pressure in the injection volume is proportional to amount. The grey bar indicates the typical sample size range extracted from ice samples. B) Calibration curve; known CO_2 mixing ratios of air standards vs. ratio of IRMS peak area for CO_2 (mass 44) and TCD detected air amount transformed to pressure from the relationship shown in A.

Atmos. Meas. Tech. Discuss., doi:10.5194/amt-2015-351, 2016
Manuscript under review for journal Atmos. Meas. Tech.
Published: 1 February 2016

Atmospheric Measurement Techniques Discussions

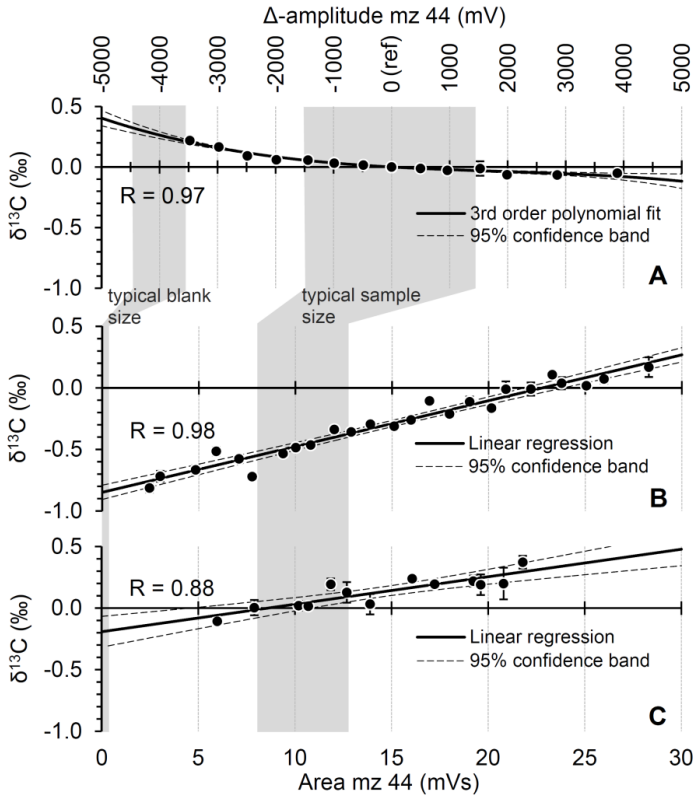

Figure 5: Fractionation effects for $\delta^{13}C$: A) IRMS nonlinearity effect; $\delta^{13}C$ dependence on peak amplitude (top x-axis), Δ–amplitude is the deviation in intensity (mass 44) from the reference peak (ref, $\delta^{13}C$ and Δ–amplitude = 0). The data is obtained from a total of 177 measurements and shown are mean values with the 1σ standard deviation. B) PreCon–GC linearity (bottom x-axis); CO_2 sample size dependence for pure CO_2 working standard directly injected to section B. The data is obtained from a total of 318 measurements corrected for IRMS nonlinearity and blank; shown are mean values with the 1σ standard deviation. C) Air amount dependence (bottom x-axis); air sample size dependence for air standards/samples injected to section A. The data is obtained from a total of 46 measurements corrected for IRMS nonlinearity, PreCon–GC linearity and system blank, shown are mean values with the 1σ standard deviation. The grey bars indicate the typical procedural blank and sample size range of air extracted from ice samples, respectively.

Atmos. Meas. Tech. Discuss., doi:10.5194/amt-2015-351, 2016
Manuscript under review for journal Atmos. Meas. Tech.
Published: 1 February 2016

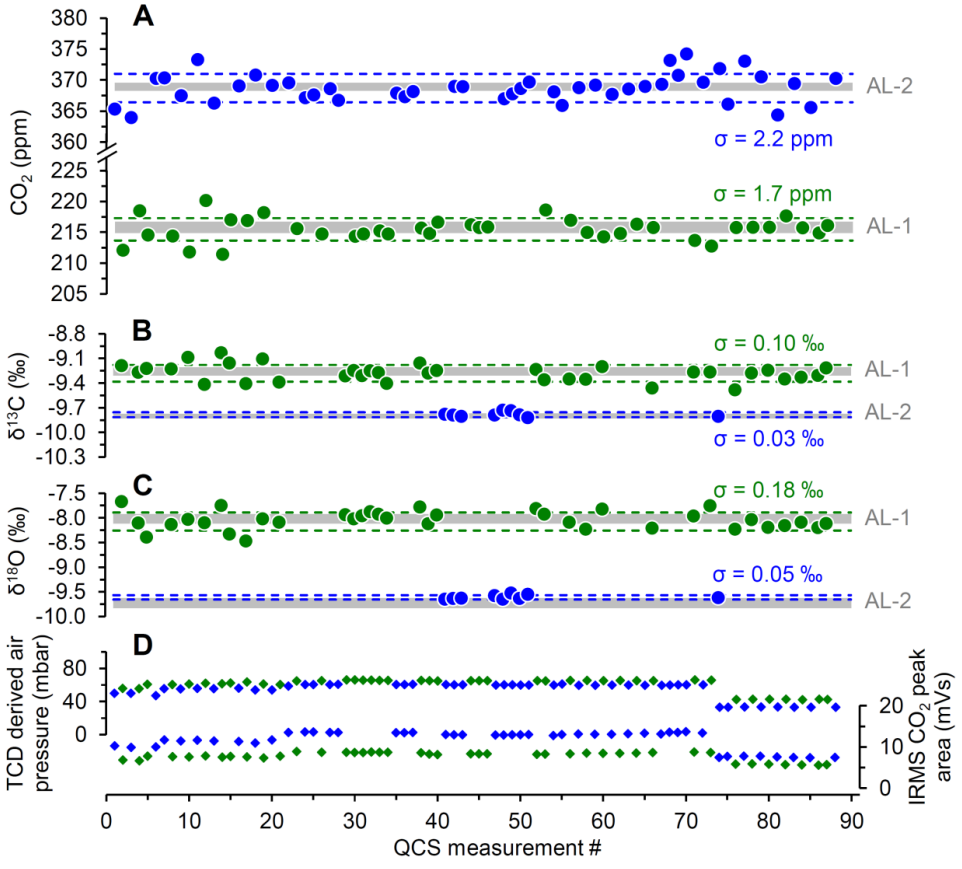

Figure 6: Repeated quality control sample (QCS) measurements of air standards AL–1 (in green) and AL–2 (in blue) over ice, covering a time period of two years. The grey bands indicate the assigned value of the standard with uncertainty as given in Table 1. Dashed lines indicate the 1σ standard deviation of the data points (see numerical values). A) CO_2 mixing ratios (ppm). B) $\delta^{13}C$-CO_2 (‰ VPDB). C) $\delta^{18}O$-CO_2 (‰ VPDB-CO_2). D) Injected amount of air (top, left axis) and related amount of CO_2 (bottom, right axis). Fewer results are shown for the stable isotopes because standards used in the daily calibration routine (i.e. not post-processed similar to real samples) were excluded from this analysis.

Atmos. Meas. Tech. Discuss., doi:10.5194/amt-2015-351, 2016
Manuscript under review for journal Atmos. Meas. Tech.
Published: 1 February 2016

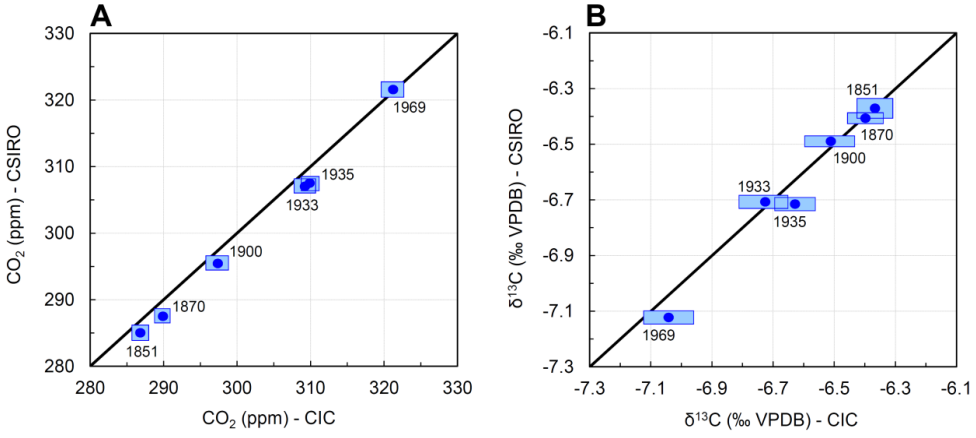

Figure 7: Laboratory intercomparison measurements between CIC and CSIRO of Law Dome ice samples covering the recent past (1851–1969 AD). Shown are CO_2 mixing ratios (A) and $\delta^{13}C$-CO_2 values (B) measured at CIC (x-axis) and CSIRO (y-axis; Rubino et al., 2013). Blue boxes indicate 1σ uncertainties defined for each laboratory by the respective side length.

Atmos. Meas. Tech. Discuss., doi:10.5194/amt-2015-351, 2016
Manuscript under review for journal Atmos. Meas. Tech.
Published: 1 February 2016

Atmospheric Measurement Techniques Discussions

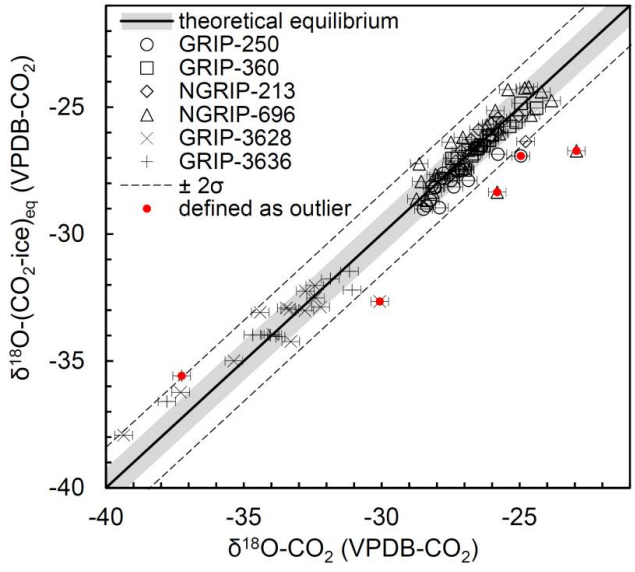

Figure 8: $\delta^{18}O\text{-}CO_2$ used as a quality control tool for ice core measurements. Shown is the correlation between measured (x-axis) and expected (y-axis) $\delta^{18}O\text{-}CO_2$ for samples from GRIP and NGRIP measured in high spatial and temporal resolution for sections (bags) with gas ages of 260 to 1770 years and 25'000 years. The expected $\delta^{18}O\text{-}CO_2$ was derived considering thermodynamic equilibrium of gaseous CO_2 with the surrounding ice matrix and is accordingly denoted as $\delta^{18}O\text{-}(CO_2\text{-ice})_{eq}$ (see text for details). The calculated theoretical equilibrium (black line) is shown with an uncertainty band (grey) accounting for the error associated with equilibrium temperature estimates. The dashed line indicates the 2σ standard deviation around the theoretical value considering all data points shown. For samples outside this range (red circles) CO_2 and $\delta^{13}C\text{-}CO_2$ results were rejected.